

ALPHA LABORATORY IMMERSION

Bethel University, 6/26 – 6/28/2012 — 1 setup

Plasmonics and Surface-Enhanced Spectroscopy

Description:

Metallic nano-structures made from gold or silver display unusual optical properties not found in natural materials. This is due to the abundance of free electrons that are free to wiggle and propagate as plasmon waves. The rapidly emerging field of “plasmonics” is leading to significant new discoveries and numerous applications. In particular, plasmon waves give rise to extremely intense and localized optical fields. These can be exploited for surface-enhanced spectroscopy and biosensing.

Participants will be using a home-made laser scanning microscope. Based around a commercial Nikon microscope, a spectrometer, a HeNe laser, and sets of spectroscopy filters, participants will explore basic microscopy imaging techniques, laser-induced fluorescence, Raman spectroscopy, and chemical imaging of surfaces at micrometer scales. The participants will then explore the generation and exploitation of plasmons for surface-enhanced Raman spectroscopy (SERS). SERS is powerful optical biosensing and chemical identification technique, providing unique molecular “fingerprints,” and has received significant attention.

The immersion experiments would cover use of the microscope system, fabrication of low-cost plasmonic substrates, formation of molecular monolayers for SERS analysis, and spectroscopic chemical imaging of the SERS substrates. Time will also be spent exploring and customizing the microscope and laser setup. The microscope system has been used successfully by physics students (imaging, optical tweezers, metrology) as well as by chemistry and biology students (Raman identification of unknown samples, optical tweezing, fluorescence imaging).

Participants should bring a lab notebook. Safety concerns: using lasers in a microscopy setup.

Mentors – Bio

Name/Title: Nathan C Lindquist, Assistant Professor of Physics

Email Address: n-lindquist@bethel.edu Phone: 651-638-6513

Institution Name: Bethel University Dept.: Physics

Mailing Address: 3900 Bethel Drive, St Paul MN 55112

Street, City, State, Zip

BS (Physics) Bethel University, MS (Physics) U of Minnesota, PhD (Electrical Engineering) U of Minnesota.



During his PhD and postdoctoral studies, Nathan researched interdisciplinary applied optics and nanotechnology. His research experience includes areas such as plasmon-enhanced solar cells, nano-optical bio-sensors, nano-optical data storage and devices, plasmon-enhanced spectroscopy, and novel nano-fabrication techniques. In his labs at Bethel, he tinkers with lasers, microscopes and molecules, and continues research in nanotechnology, plasmonics, optical biosensing, microfluidics, and "lab-on-a-chip" technologies.

- 1. Experiment 1: Excitation of “Surface Plasmon Resonance” in a 50 nm thick gold film**
 - a. Using the “Kretschmann Prism Coupling” setup, we will produce evidence of surface plasmon excitation
 - i. By tuning the angle of illumination in a total internal reflection mode, evidence of plasmon excitation will show as a dark band appearing in the reflected light at only one excitation angle. A converging lens will provide multiple angles of illumination at once.
 - b. Equipment and Supplies
 - i. 50 nm thick gold chip (commercially available)
 - ii. HeNe laser
 - iii. Right-angle prism
 - iv. Linear polarizer
 - v. Converging lens ($f \sim 6$ cm)
 - vi. Microscope index matching immersion oil
 - vii. Various optomechanics, especially a rotating stage
 - viii. Viewing screens
 - c. Procedure
 - i. Setup the laser → polarizer → converging lens → prism → two viewing screens
 - ii. The prism is mounted on a rotating stage
 - iii. Fix the gold-coated coverslip to the prism with a drop of immersion oil
 - iv. The converging lens is focused onto the gold film through the prism in a total internal reflection mode
 - v. A dark band will appear in the reflected light indicating the plasmon resonance
 - vi. Changing the polarization (s vs p) will allow viewing of the plasmon band
- 2. Experiment 2: Excitation of “Localized Surface Plasmon Resonance” in 60 nm gold nanoparticles**
 - a. Using a solution of 60 nm gold nanoparticles in water, we will measure an ensemble average absorption spectrum.
 - i. The free-electron could (jellium) of a sphere has a particular resonance frequency
 - b. Equipment and supplies
 - i. 60 nm gold nanoparticles (commercially available)
 - ii. Micropipettes and cuvette
 - iii. Cuvette holder
 - iv. White light source
 - v. Spectrometer
 1. Economical Ocean Optics USB4000 (fiber coupled)
 - c. Procedure
 - i. Fill the cuvette with the stock solution of nanoparticles
 - ii. Pass white light through the cuvette and into a spectrometer
 - iii. Remove the cuvette and capture a reference white light spectrum
- 3. Experiment 3: Excitation of a “Localized Surface Plasmon Resonance” from a single nanoparticle**
 - a. Using a solution of 60 nm gold nanoparticles, we will show evidence of a localized plasmon resonance mode
 - i. The free-electron could (jellium) of a sphere has a particular resonance frequency
 - ii. Examining a single nanoparticle can show distinct differences in the size and shape
 - b. Equipment and Supplies
 - i. 60 nm gold nanoparticles (commercially available)
 - ii. Micropipettes
 - iii. Glass coverslips
 - iv. White light source
 - v. Darkfield microscope for single particle analysis (**Figure 1**)
 - vi. Spectrometer attached to the microscope output
 - c. Procedure
 - i. Deposit 30 μL of stock nanoparticle solution on a glass coverslip and allow to air dry

- ii. Find a single nanoparticle in the darkfield microscope
 - 1. The particles will be many colors. Look for a single red dot. Other colors correspond to pairs and clumps of nanoparticles.
 - iii. Measure the scattering spectrum of the nanoparticle using the spectrometer
- 4. Experiment 4: Surface-enhanced Raman spectroscopy (SERS) from a single nanoparticle**
- a. Using the darkfield microscope setup, we will measure a SERS signal from a single gold nanoparticle deposited on a coverslip
 - i. The localized plasmon resonance from the gold nanoparticle will greatly increase the electromagnetic field intensity giving a million-fold increase in the Raman signal
 - b. Equipment and supplies
 - i. 60 nm gold nanoparticles (commercially available)
 - ii. Benzenethiol solution, diluted (CAUTION: TOXIC!)
 - iii. Micropipettes
 - iv. Glass coverslips
 - v. HeNe Laser
 - vi. Brightfield microscope with laser illumination
 - vii. Laserline filter, dichroic beam-splitter, and steep long-pass filter
 - viii. High-sensitivity spectrometer
 - c. Procedure
 - i. Mix 300 μL of 10 mM benzenethiol with 200 μL of stock nanoparticle solution
 - 1. Allow \sim 30 minutes to allow the benzenethiol to bind to the nanoparticles
 - ii. Deposit 30 μL of the solution on a glass coverslip and allow to dry
 - iii. Find a single nanoparticle in the darkfield microscope (**Figure 2**)
 - iv. Measure the SERS spectrum of the scattered light in the spectrometer by using the HeNe laser source and the long-pass filters
- 5. Experiment 5: Scanning the laser source to form a “Chemical Image” of a surface**
- a. Using the microscope system, we can also scan the laser source and gather a full Raman (or SERS) spectrum at every point. With this setup, a chemical image of the surface can be formed.
 - b. Equipment and supplies
 - i. In addition to the microscope system used in the above experiments, the microscope needs to be fitted with a nanopositioning stage.
 - c. Procedure
 - i. The same as gathering a single Raman or SERS spectrum (**Figure 3**), only this time the sample is scanned under the beam (**Figure 4**).

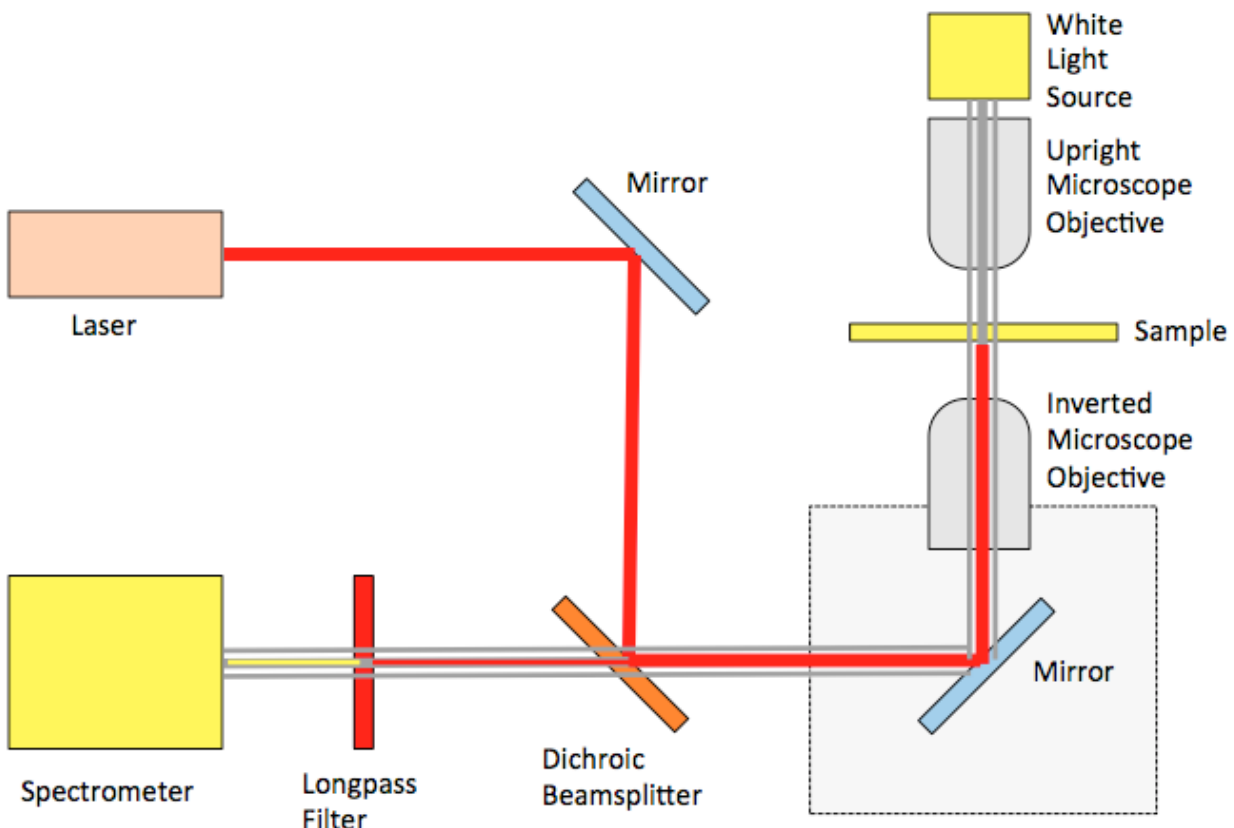


Figure 1: Schematic of the microscope system. Both white light scattering, reflection and transmission spectra can be taken as well as laser-induced fluorescence or Raman scattering.

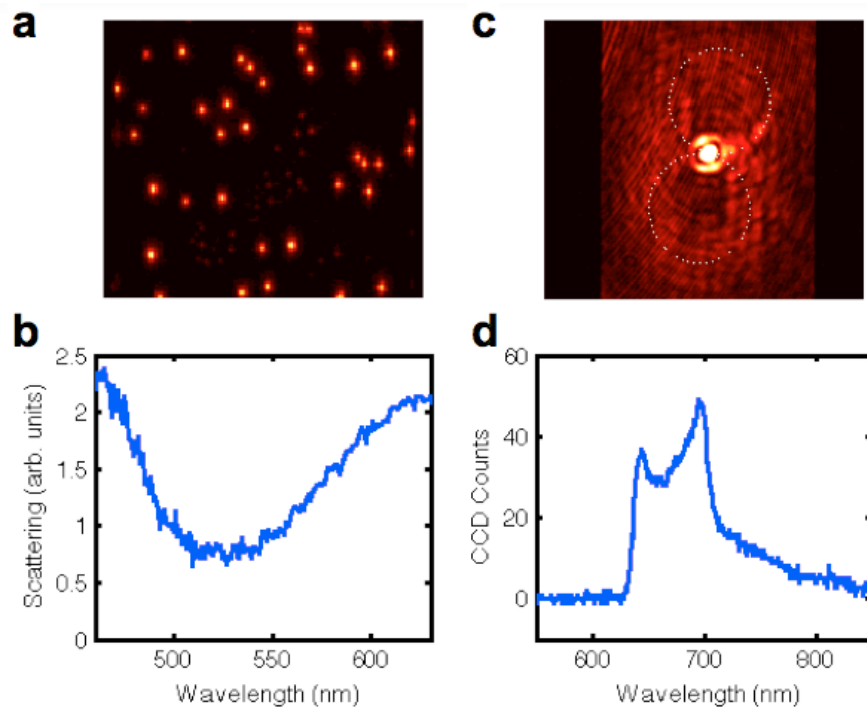


Figure 2: Single nanoparticle characterization. (a) Darkfield image of 60 nm gold nanoparticles on a glass cover slip. (b) Scattering spectrum of a single gold nanoparticle. A clear plasmon resonance near 530 nm is seen. (c) Farfield dipole scattering image from a single nanoparticle. A 633 nm laser is focused onto the particle. The particles have been coated with benzenethiol. (d) Examining the scattered light in a spectrometer reveals a SERS spectrum of the benzenethiol molecules.

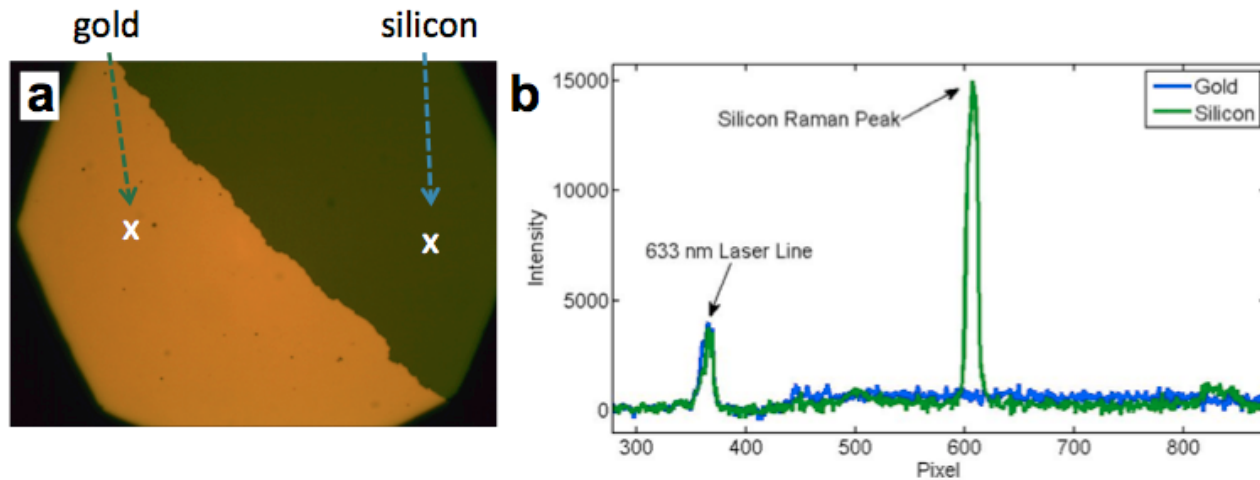


Figure 3: Single point chemical imaging. (a) With the laser over either a gold or a silicon portion of a sample, (b) clear differences in the collected Raman spectra are seen.

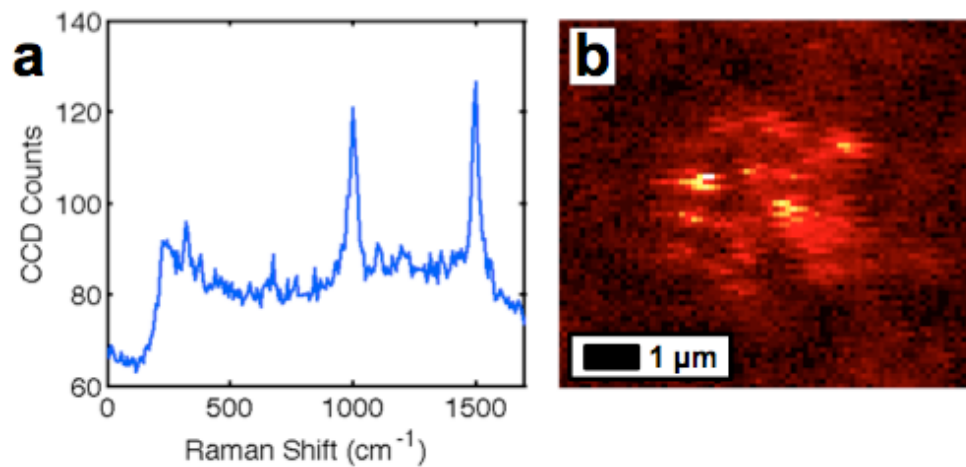
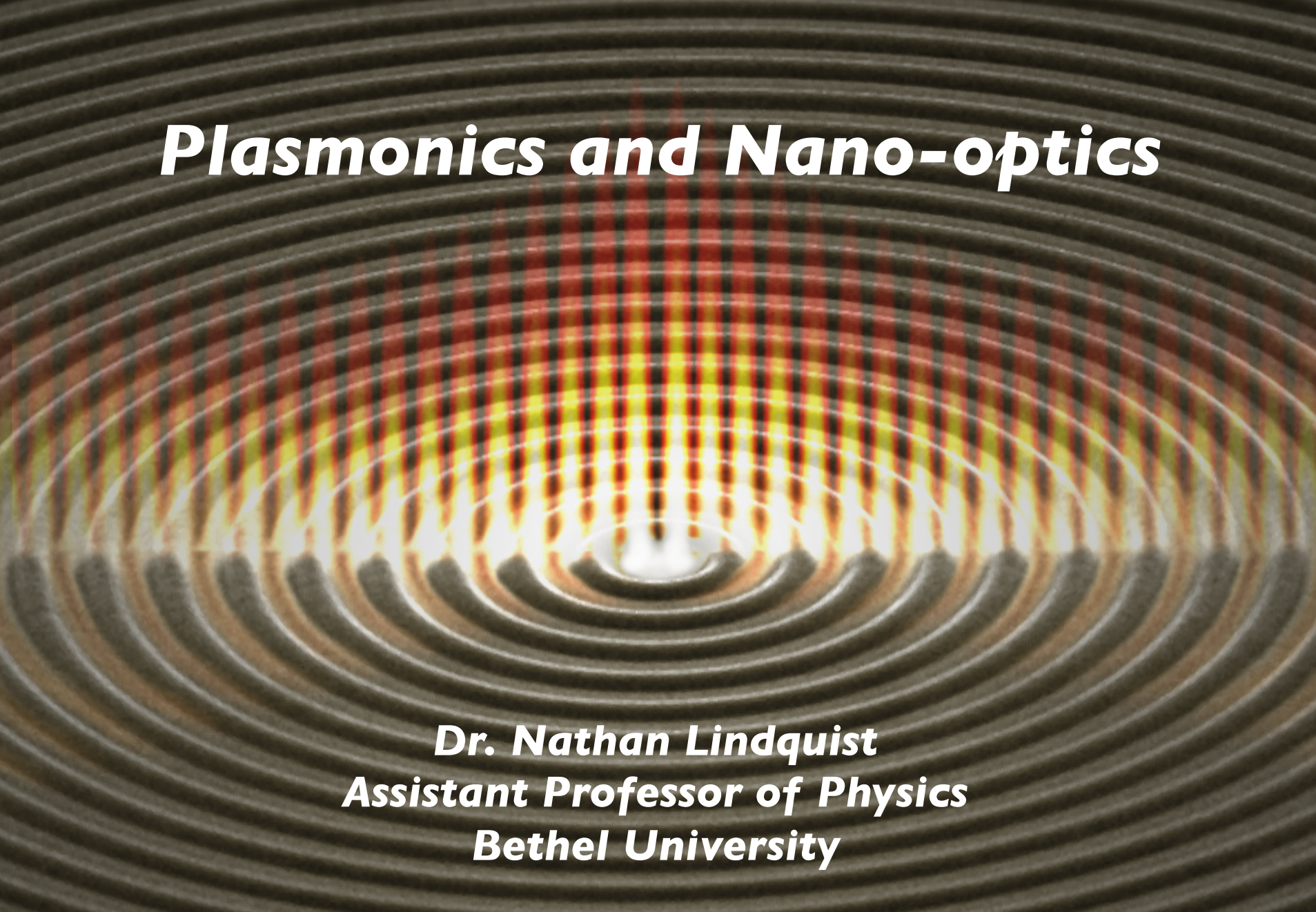


Figure 4: Scanning chemical imaging with SERS. (a) A representative SERS spectrum from a monolayer of benzenethiol molecules adsorbed on the surface of a roughed silver sample. (b) Scanning the laser over a small region produces a chemical image. The map is produced by taking the intensity of the peak at 1000 cm^{-1} .

Plasmonics and Nano-optics



***Dr. Nathan Lindquist
Assistant Professor of Physics
Bethel University***

Light and Nanotechnology

■ Motivation:

- Understatement: light is an extremely useful form of energy.
- Nanotechnology is a rapidly emerging field with the potential to “revolutionize everything.”
- Can we use these two together?

Nanotechnology Length Scales

“Meter” : “Millimeter” : “Micrometer” : “Nanometer”



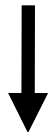
Human



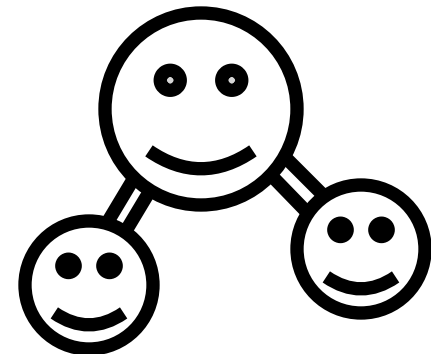
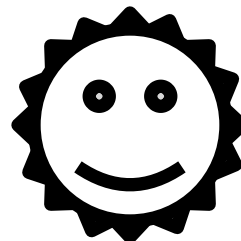
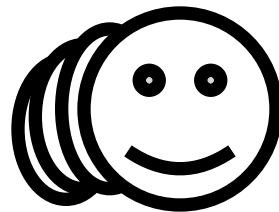
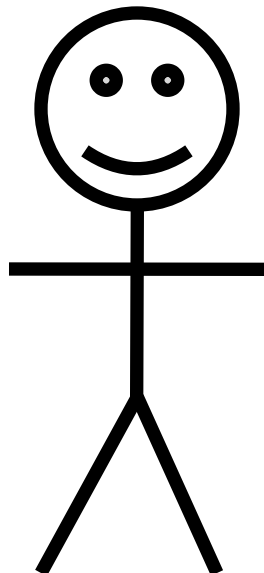
Tiny Bug



Single Cell



Single Molecule



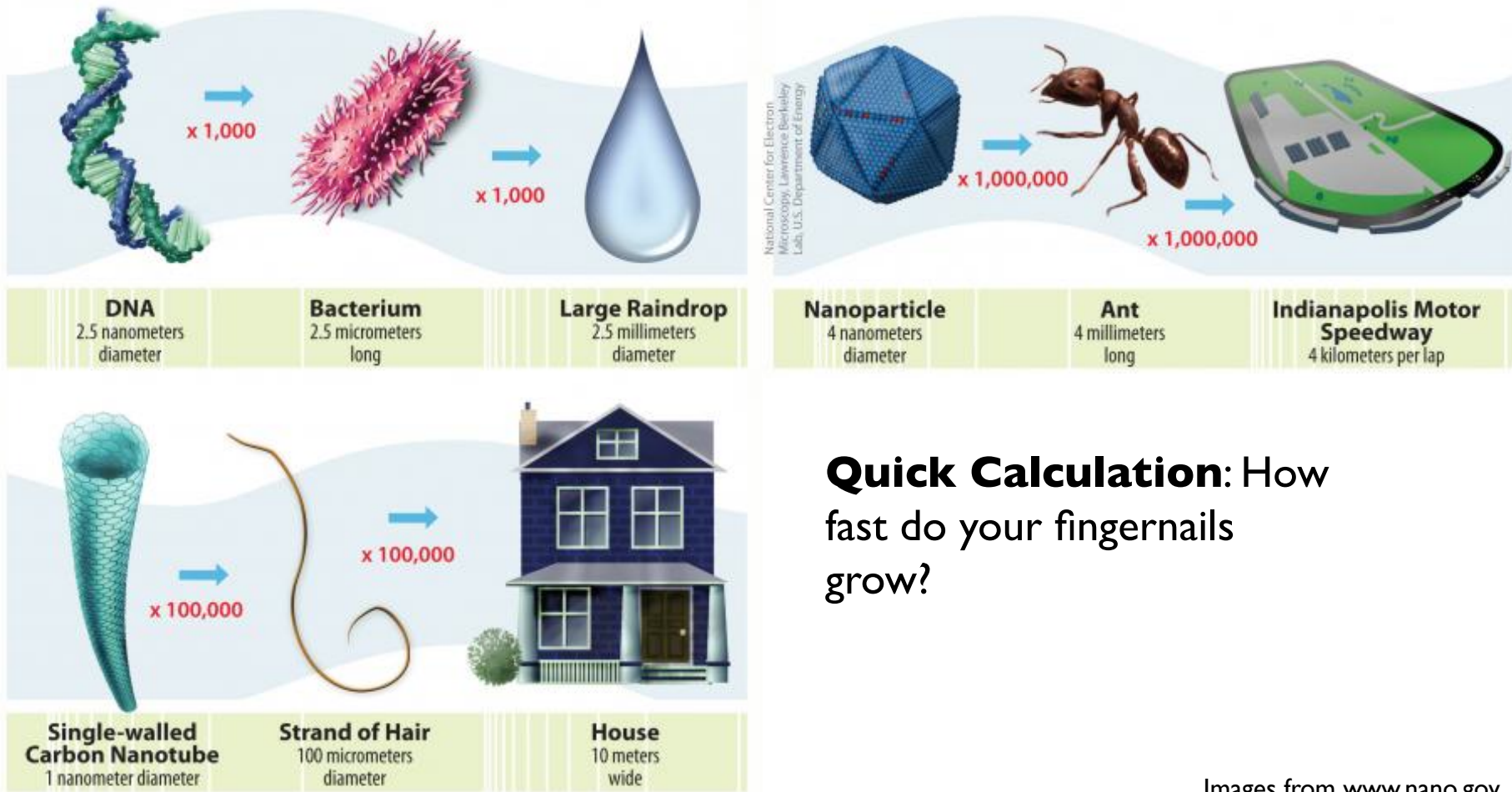
“New York to LA”

“2 ½ miles”

“13 feet”

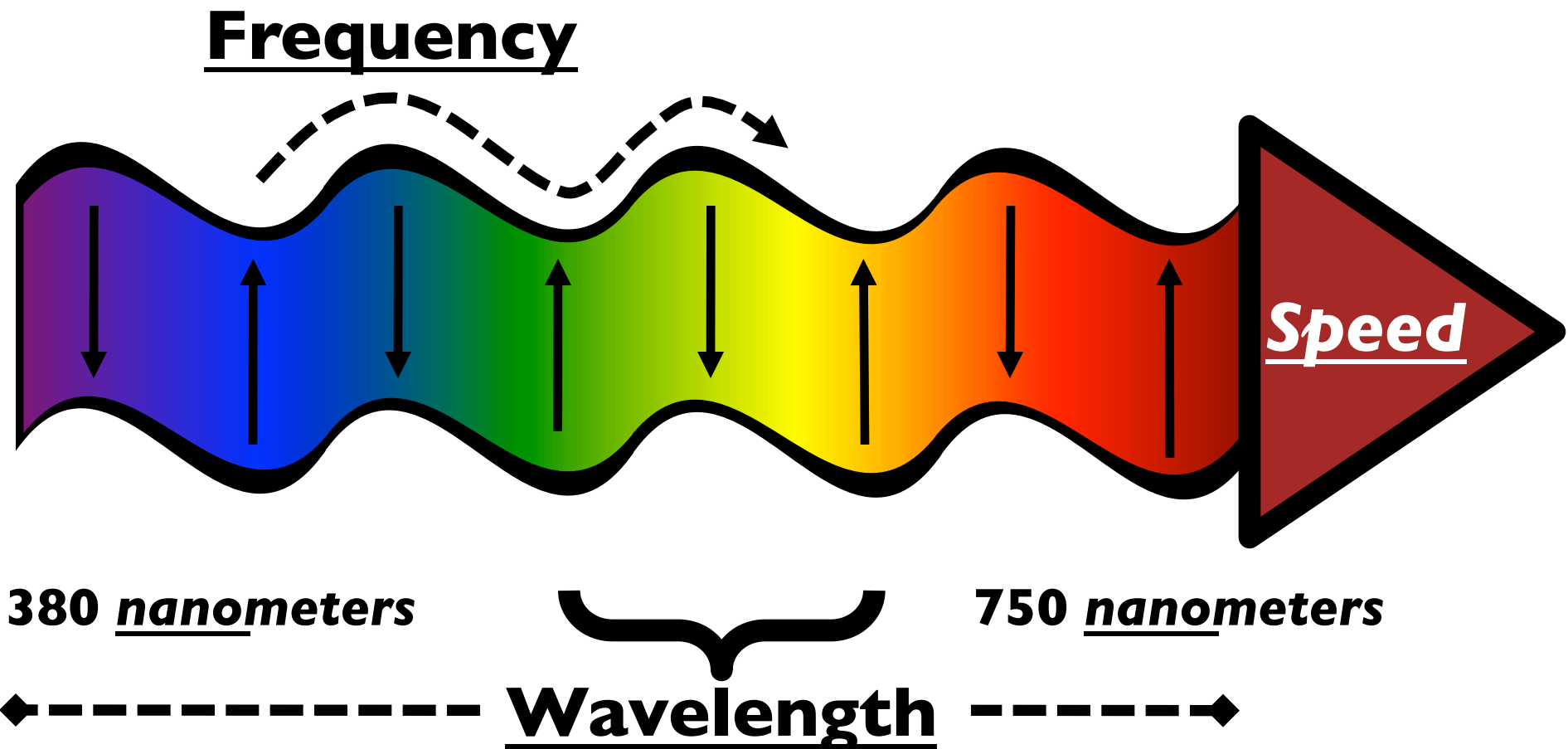
“0.1 inch”

Nanotechnology Length Scales



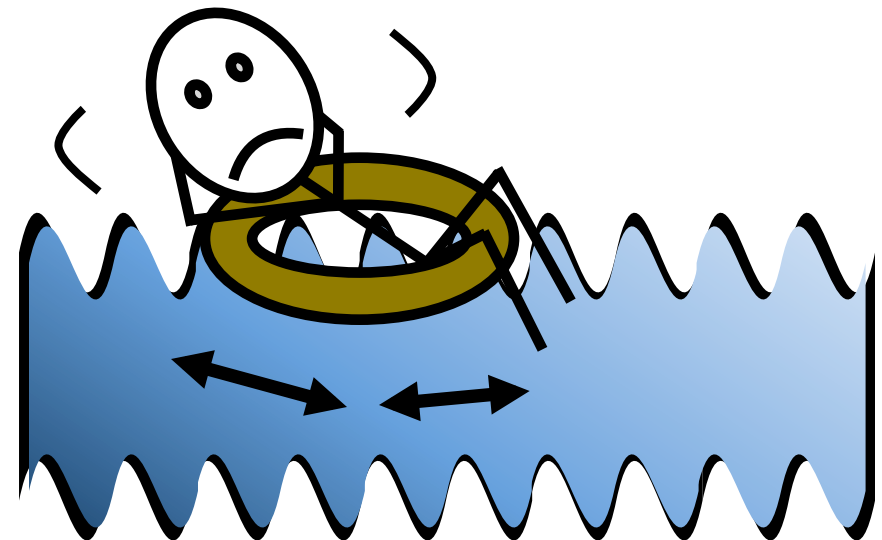
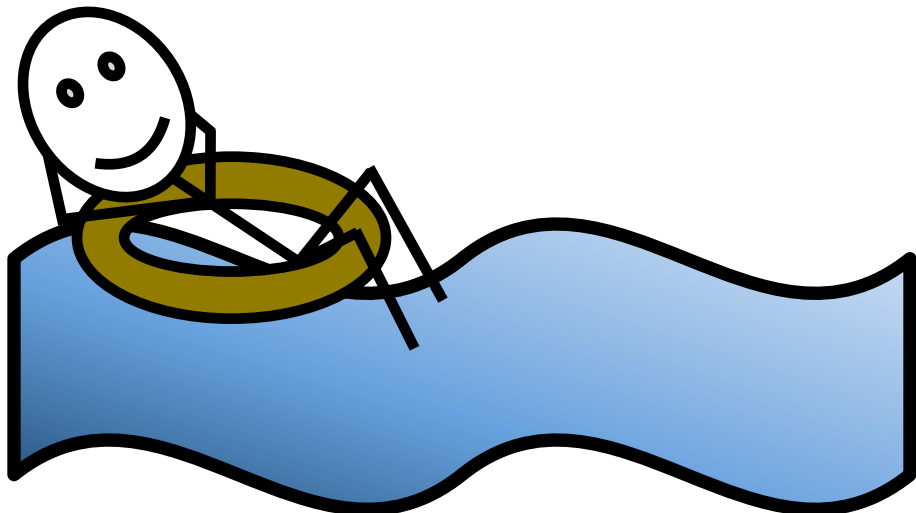
Images from www.nano.gov

Light: an Electro-Magnetic Wave



Light and the “Diffraction Limit”

Working with waves has a fundamental limit:



Wavelength > Object
Waves aren't disturbed by object too much, object slips by undetected!

Wavelength < Object
Waves are disturbed by object, deflected waves are “seeing” it!

Light and the “Diffraction Limit”

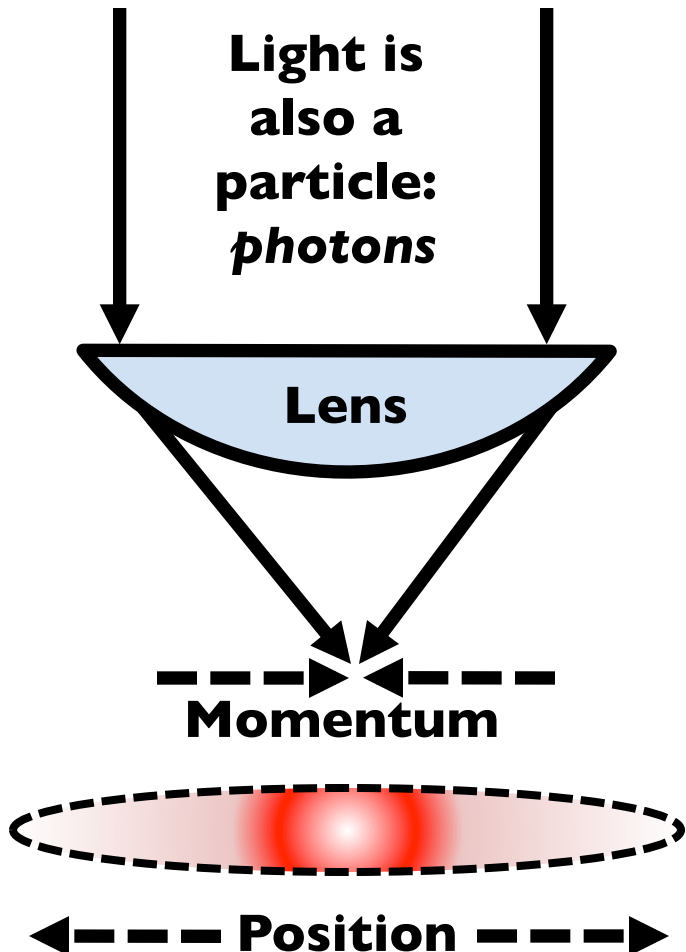
Working with *particles* has a fundamental limit:

Heisenberg's Uncertainty Principle:

The more we know about a particle's momentum, the less we know about its position.

Powerful microscopes, with a very tight focus, cannot get rid of this “smearing”.

$$\Delta x \approx \lambda/2$$

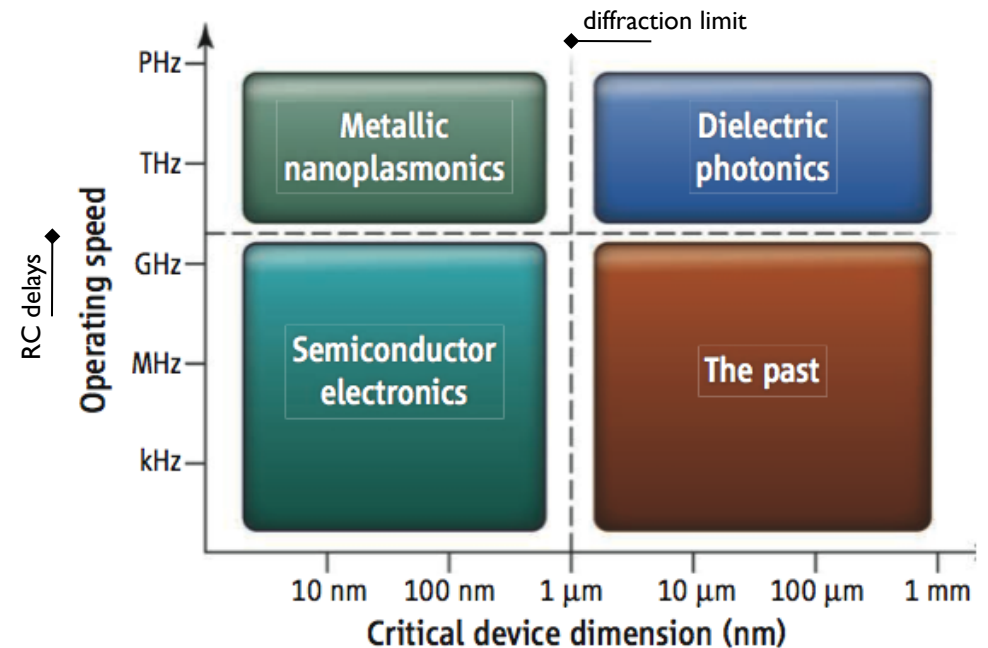


Plasmonics and Nanotechnology

- “Plasmonics” promises to break the diffraction limit by using **photons** that are mixed with **electrons**:
 - **Electrons** in metals and are free to oscillate along with nearby photons (electromagnetic fields).
 - **Electrons** that are oscillating inside the metal along with **Photons** outside the metal are called **Plasmons**.
 - This wave is bound to the surface, and can be squeezed into very small volumes.
- “Plasmonics” is the merging of **photronics** and **electronics** at nanometer scales for novel devices and applications.

Plasmonics and Nanotechnology

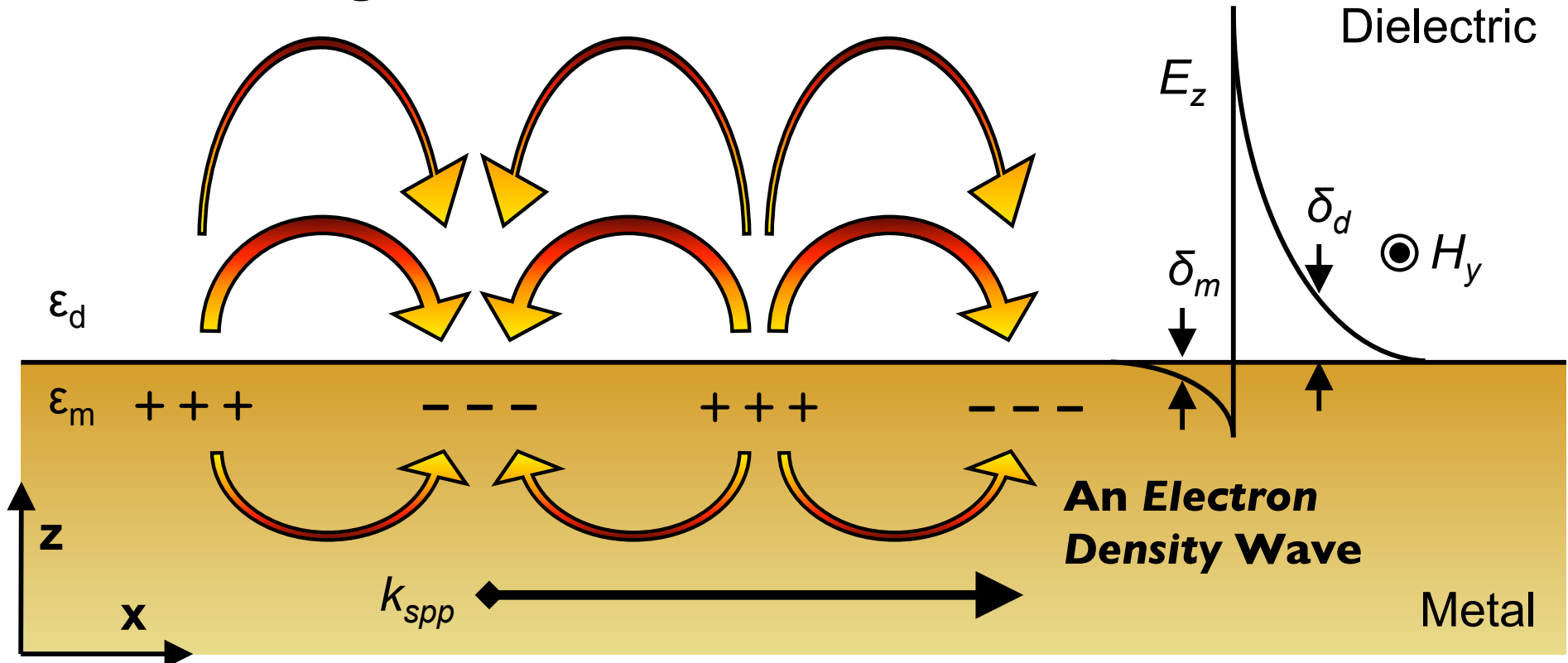
- Controlling light on nanometer scales could lead to:
 - Biosensing and enhanced spectroscopy.
 - Super-resolution imaging.
 - More efficient solar cells.
 - Optical computers.
 - Next-generation optical data storage.
 - Thermal cancer treatment.
 - Optical Cloaking.



M. L. Brongersma and V. M. Shalaev, *Science* **328** (2010)

Surface Plasmon

An Electro-Magnetic Wave



A surface wave that travels just like ripples on a pond.

Ancient Plasmonics

The “Lycurgus” Cup



Reflection

Transmission

Stained Glass Windows

The New York Times



February 21, 2005

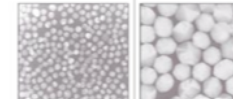
The First Nanotechnologists

Ancient stained-glass makers knew that by putting varying, tiny amounts of gold and silver in the glass, they could produce the red and yellow found in stained-glass windows. Similarly, today's scientists and engineers have found that it takes only small amounts of a nanoparticle, precisely placed, to change a material's physical properties.

Gold particles in glass

Size: 25 nm
Shape: sphere
Color reflected:

100 nanometers = 0.0001 millimeter



Silver particles in glass

Size: 100 nm
Shape: sphere
Color reflected:

20 nm

"Approximate"

Size: 50 nm
Shape: sphere
Color reflected:


Size: 100 nm
Shape: sphere
Color reflected:


Size: 40 nm
Shape: sphere
Color reflected:

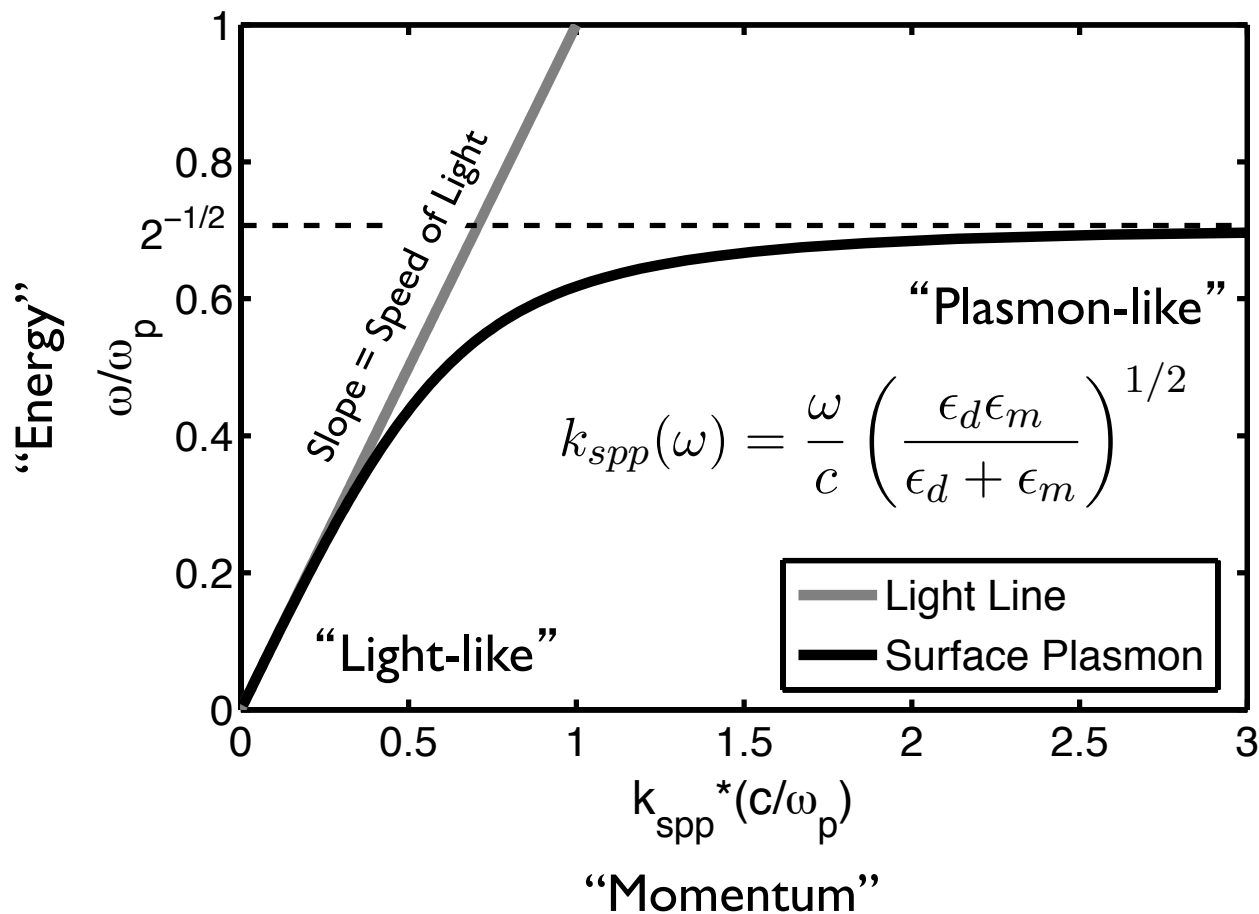

Size: 100 nm
Shape: prism
Color reflected:




The New York Times; Images courtesy of the Stained Glass Museum, Britain

Creating a Surface Plasmon

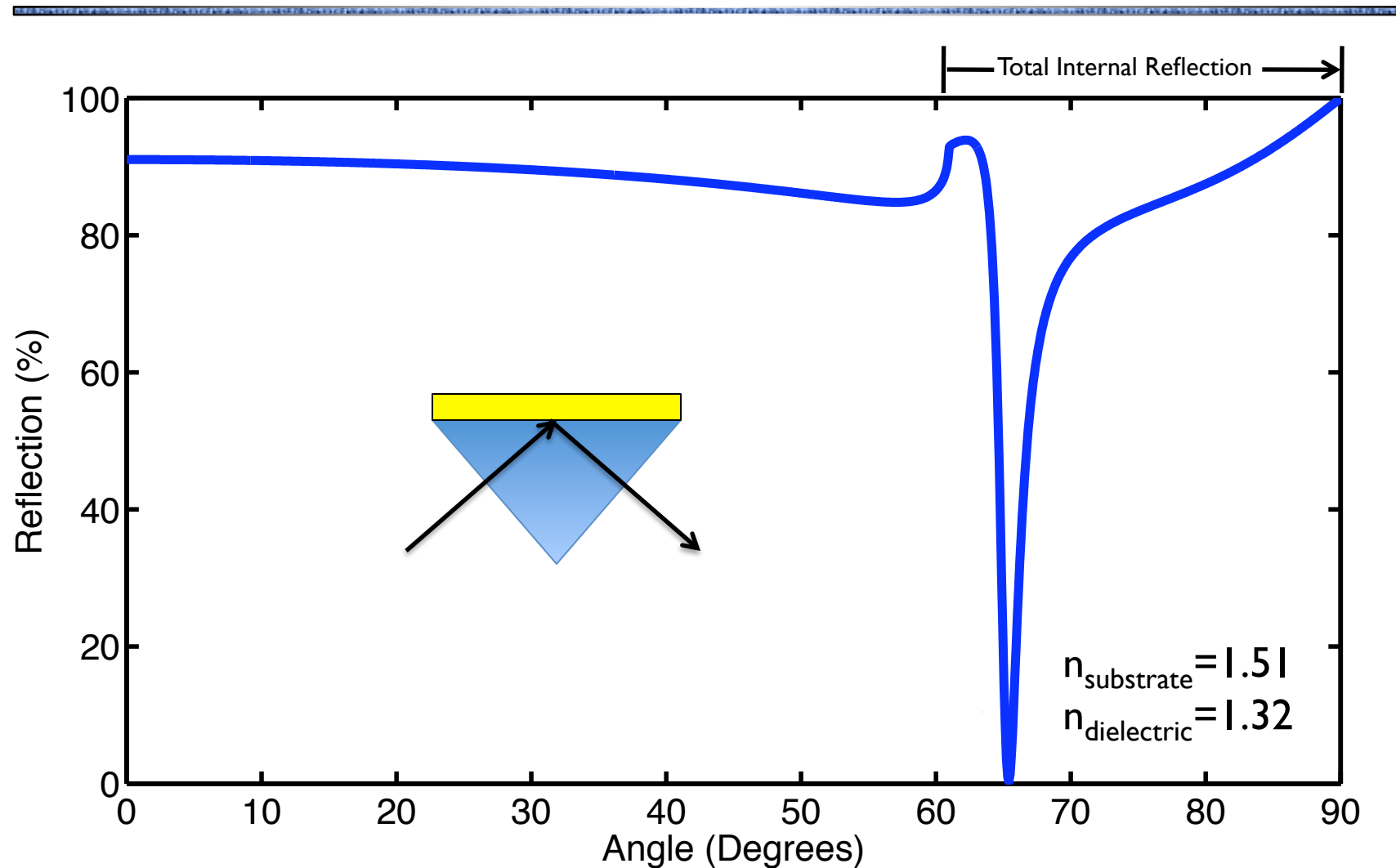
■ As always, we need to conserve energy and momentum:



There are two important ways to get that extra “momentum”

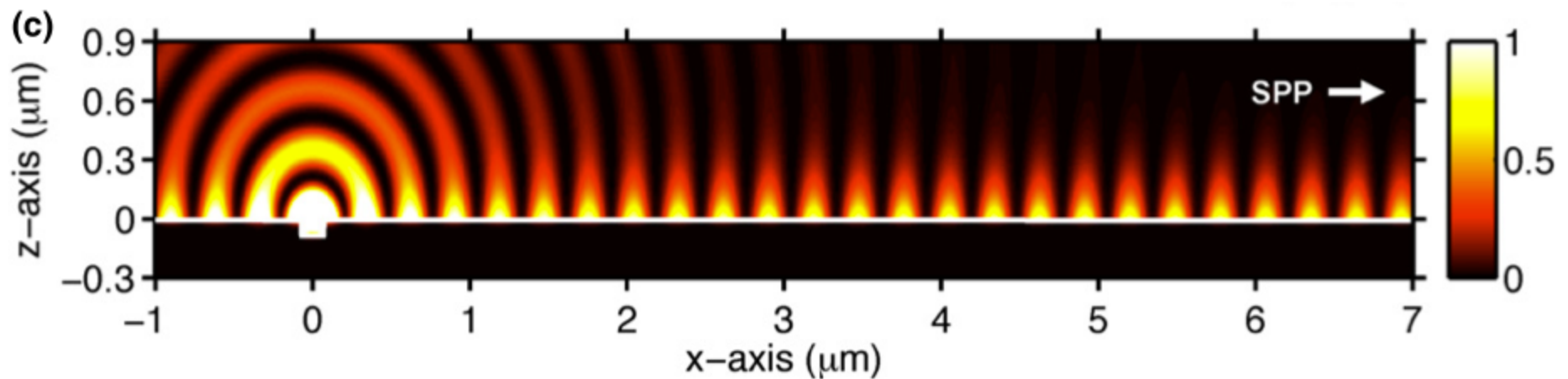
- (1) Use a chunk of glass
- (2) Use a diffraction grating

Creating a Surface Plasmon



Creating a Surface Plasmon

- Use a nano-sized bump, groove or grating on the metal surface to diffract incoming photons “into” the surface of the metal.

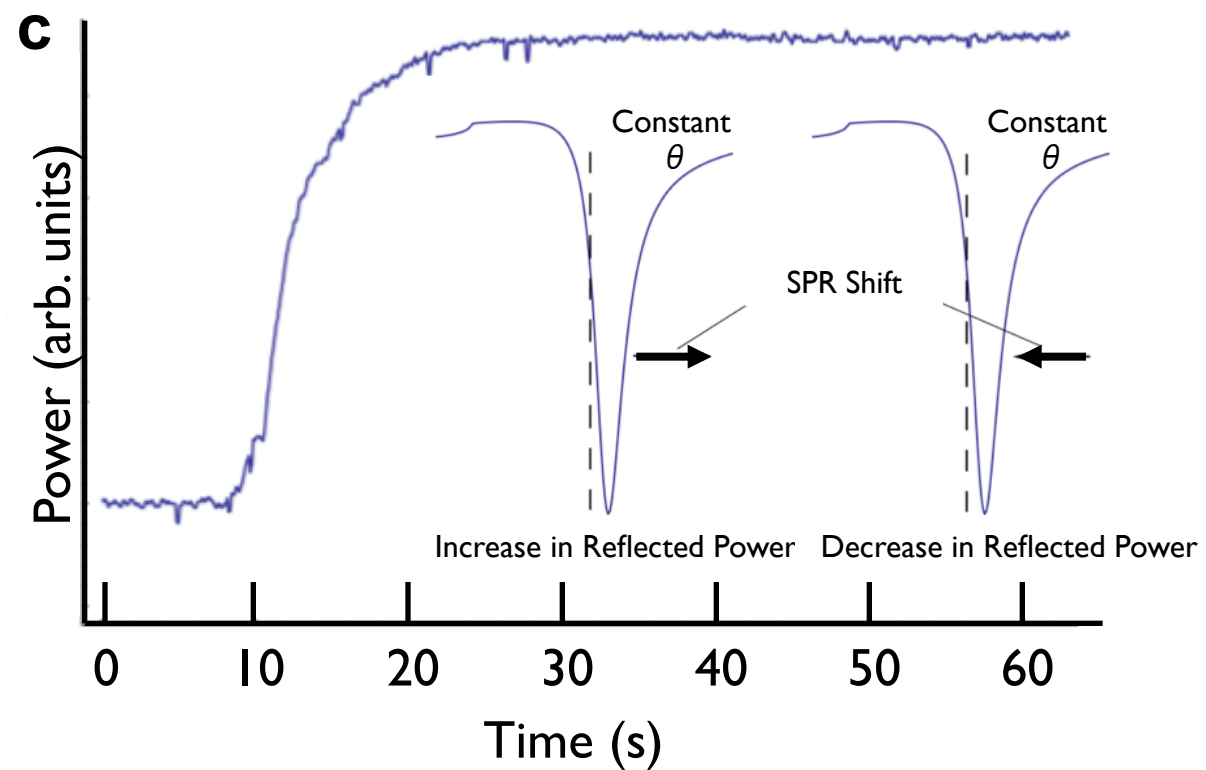
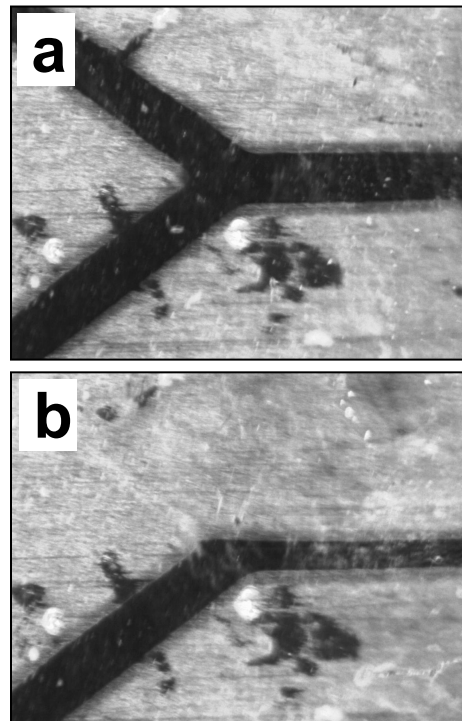


Bethel Research Background

- The high intensities of *Surface Plasmons* and their short probing range is ideal for *sensing*
- Refractive Index Sensing (Mass Sensing)
 - Molecules landing on the metal surface slightly change the refractive index and shift the resonance
- Raman Spectroscopy (Chemical Sensing)
 - Most molecules have a unique (but very weak) Raman fingerprint
 - Surface Plasmons provide Raman enhancements of $>10^6$ (or even to the \sim *single molecule* level $>10^{10}$)
 - Surface Enhanced Raman Spectroscopy (SERS)

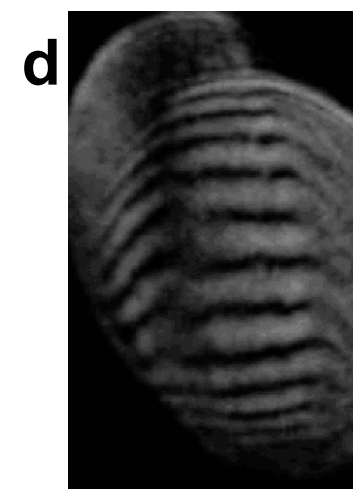
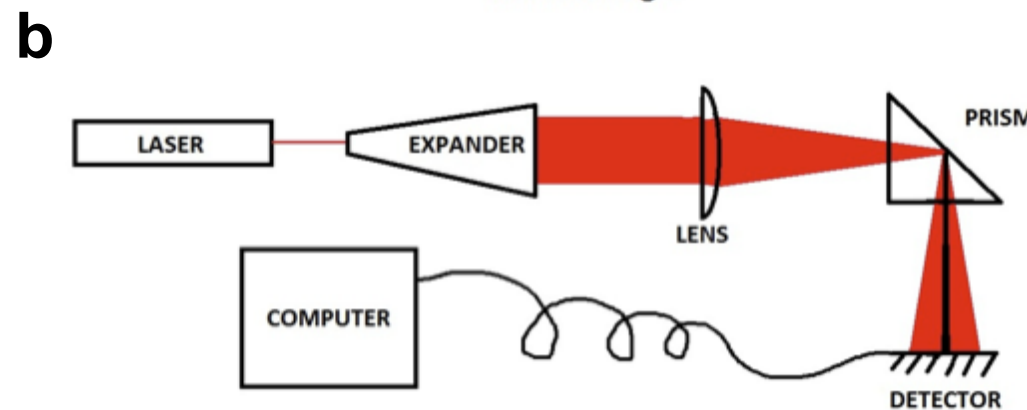
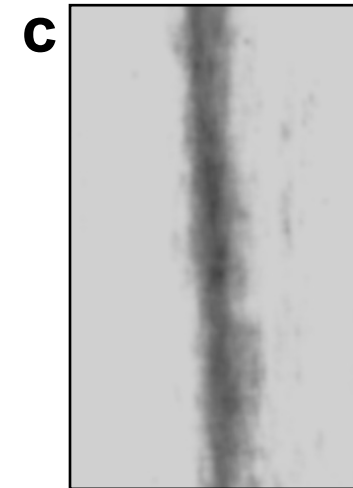
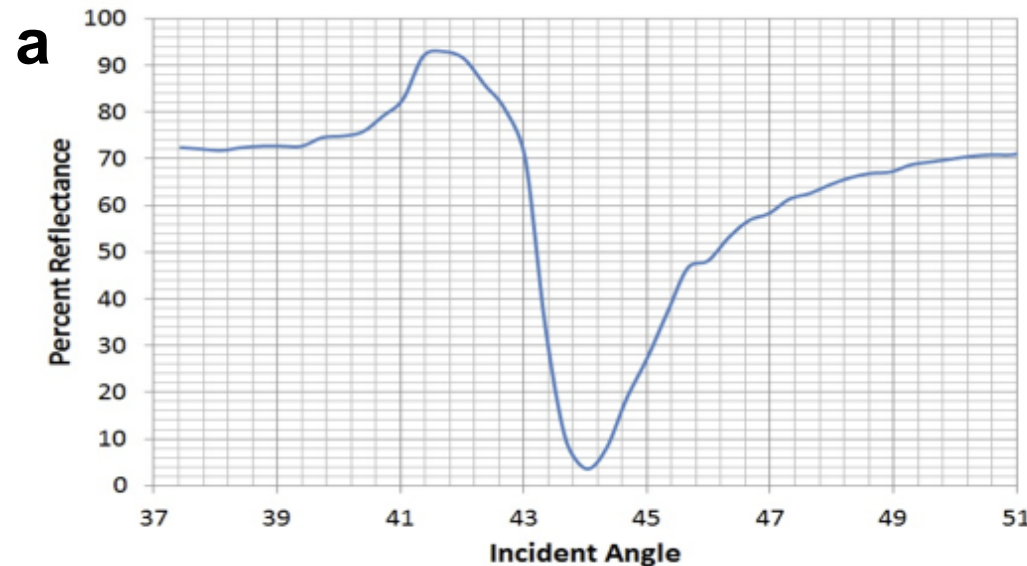
Biosensing with Surface Plasmons

■ Monitor the Surface Plasmon from a *Prism*



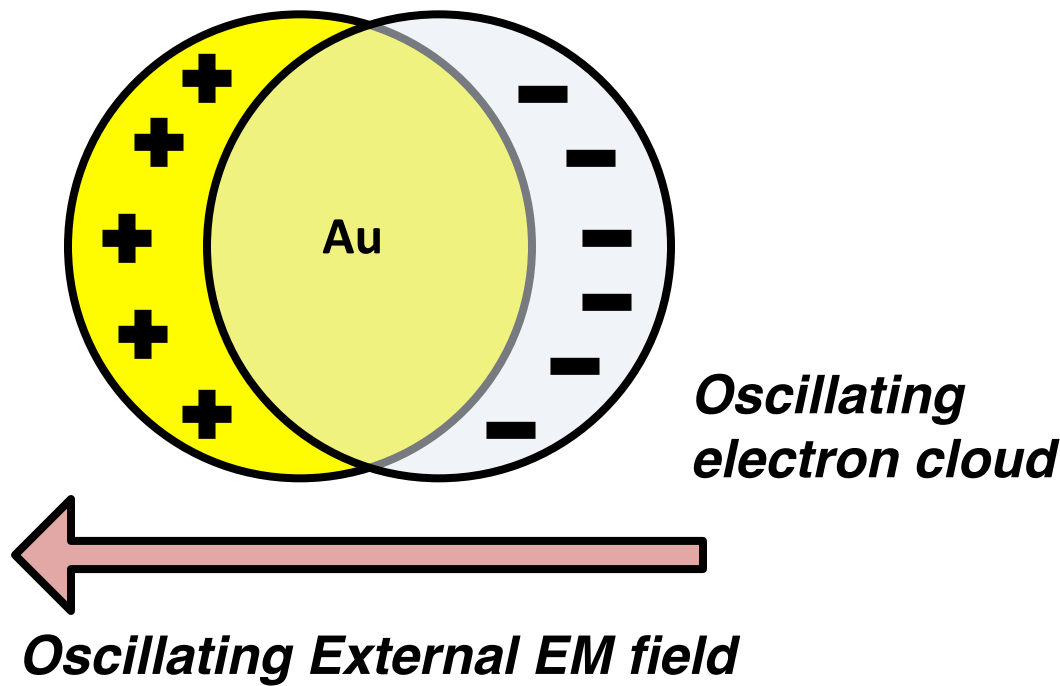
- (1) The metal film is immersed in water.
- (2) A few drops of ethanol are added, slightly changing the refractive index.

Biosensing with Surface Plasmons

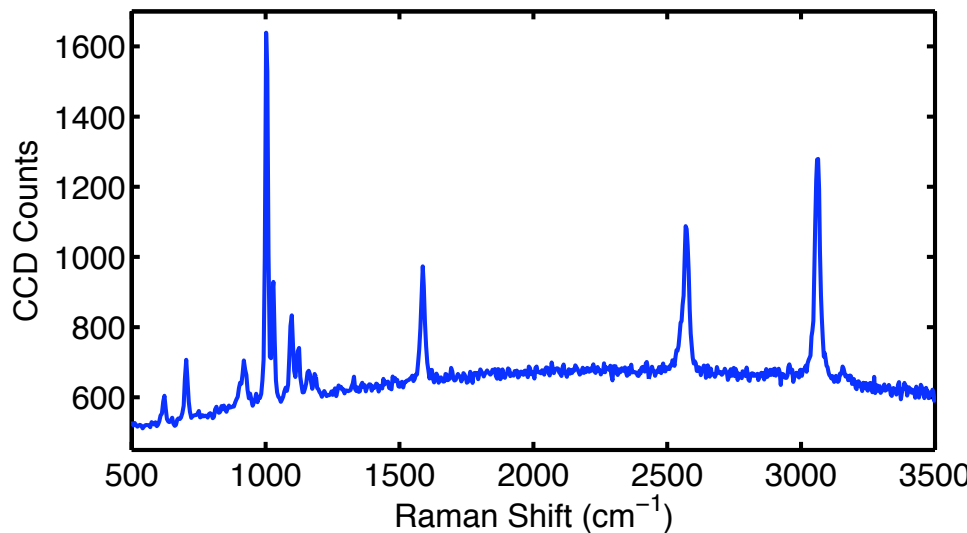
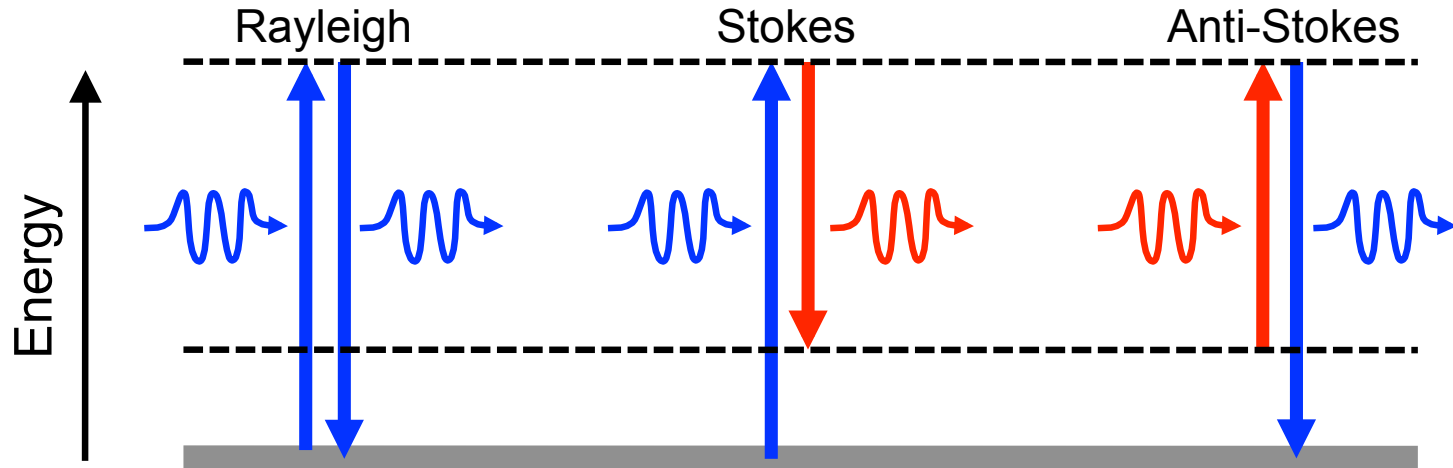


Plasmonic Nanoparticles

- In addition to *travelling SP waves*, there also exist *localized plasmons*, particularly in nanoparticles and areas of high curvature.



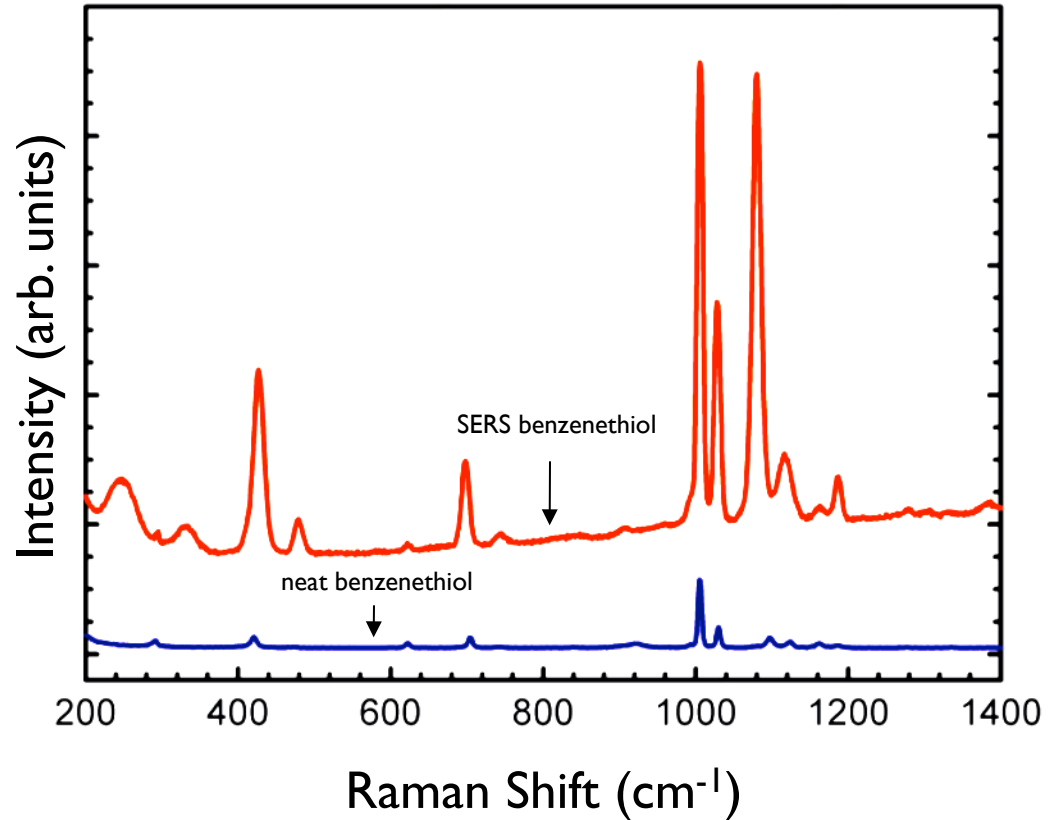
Raman Spectroscopy



Extra energy goes into exciting “phonons” of vibrational modes of the molecules. Each peak is a particular way the molecule vibrates (stretch, twist, etc...).

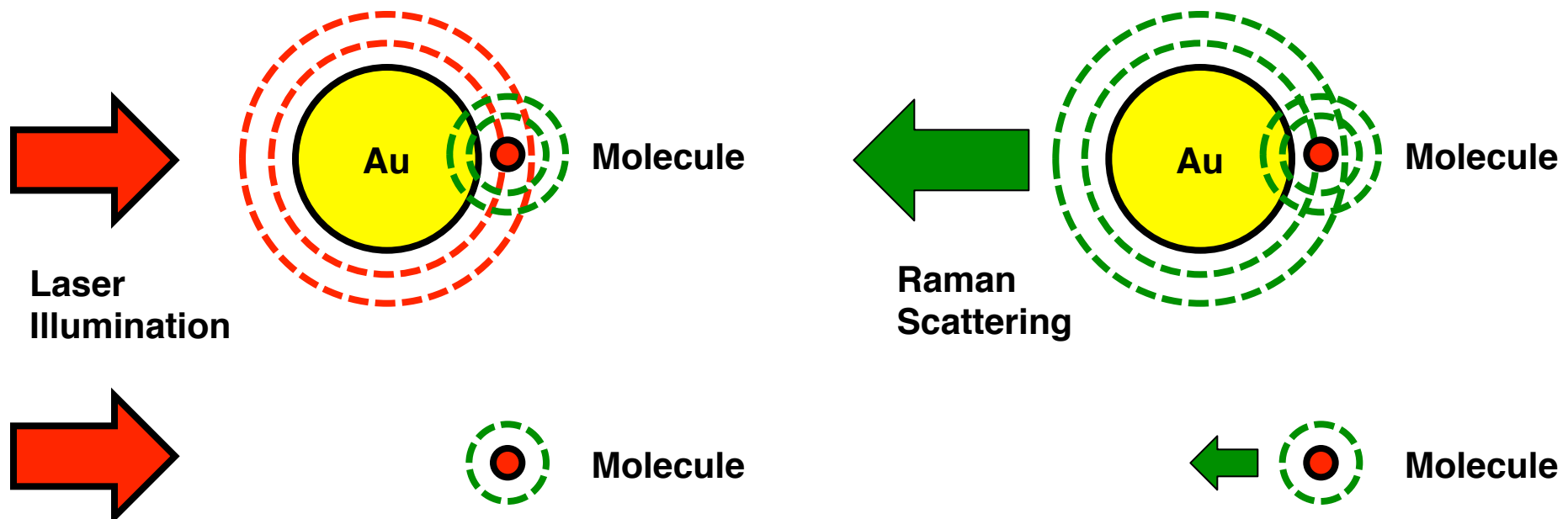
Raman Spectroscopy

- By exploiting the strong intensities of plasmons, it is possible to boost the “Raman Spectrum” or the “Chemical Fingerprint” of molecules that are on the metal surface.
- This is known as “Surface Enhanced Raman Spectroscopy” (SERS)

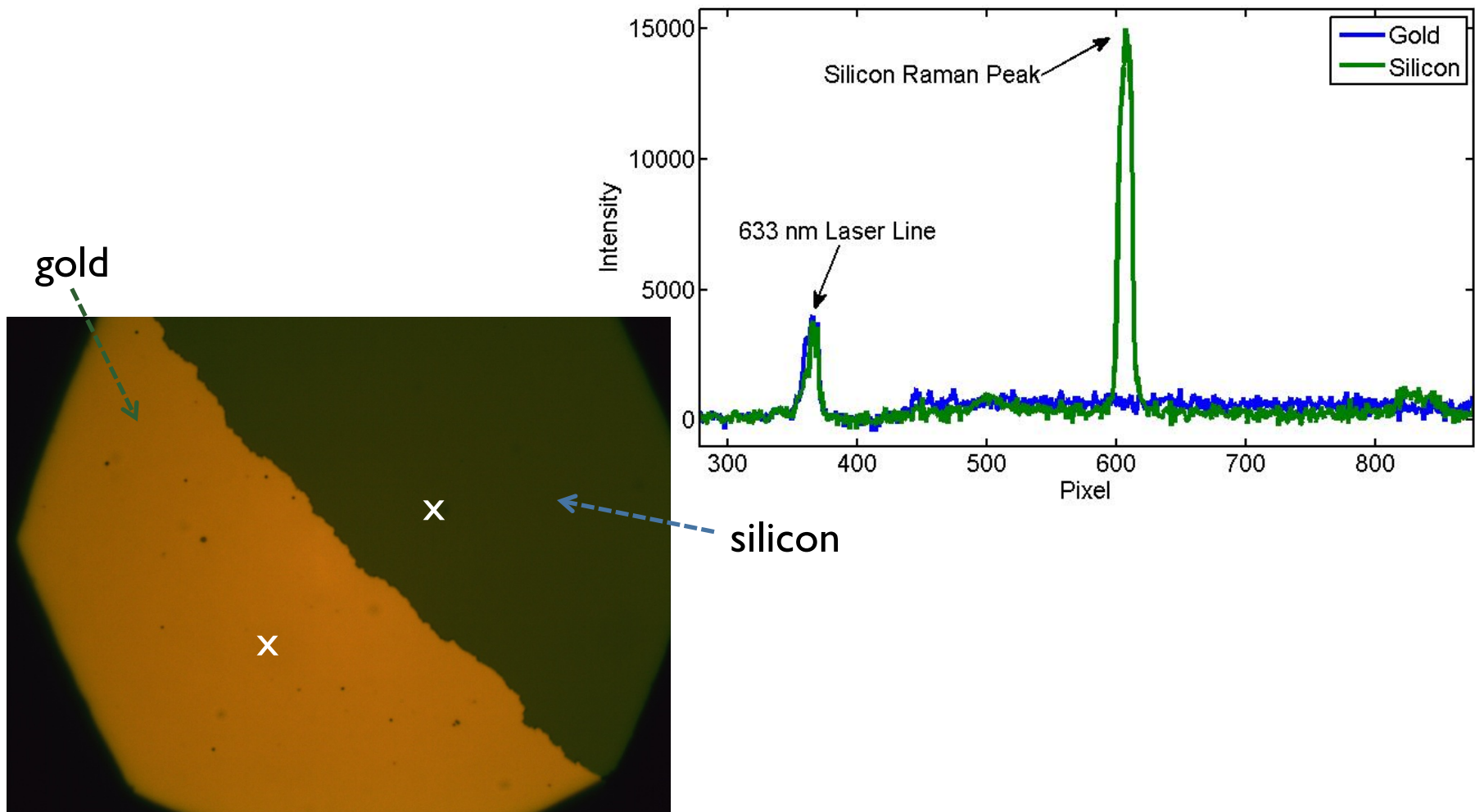


Surface Enhanced Raman Scattering

- A metallic nanoparticle acts as an antenna, both for “reception” and “transmission”
- This enhances the Raman scattering by orders of magnitude.

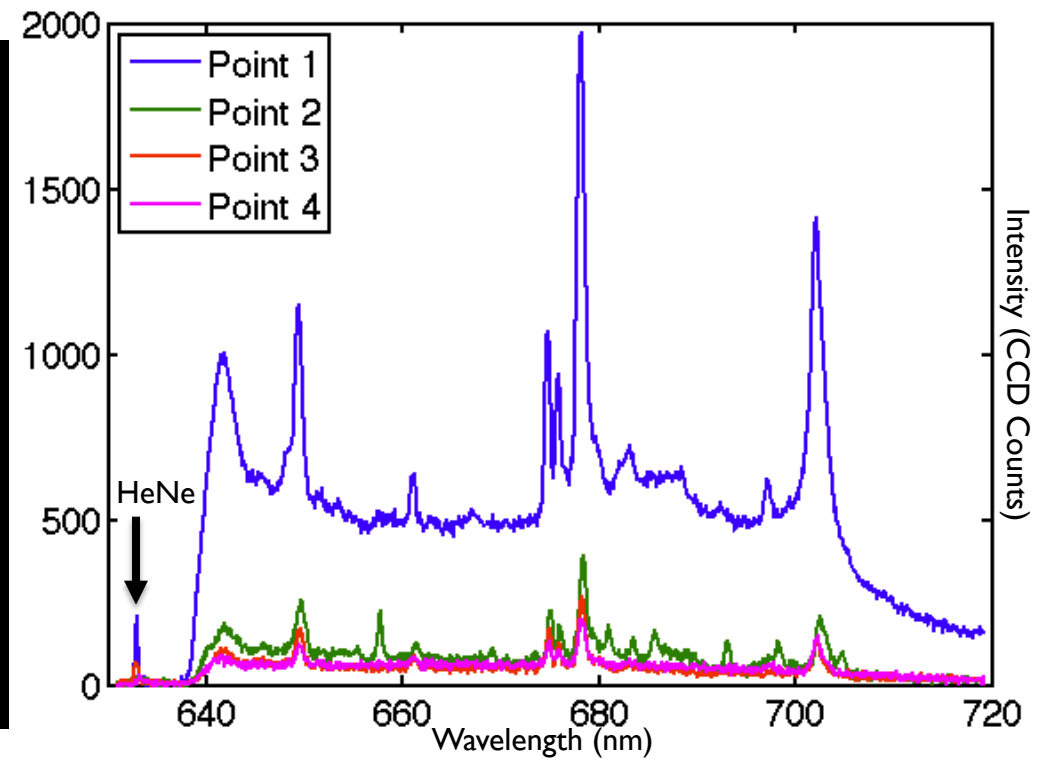
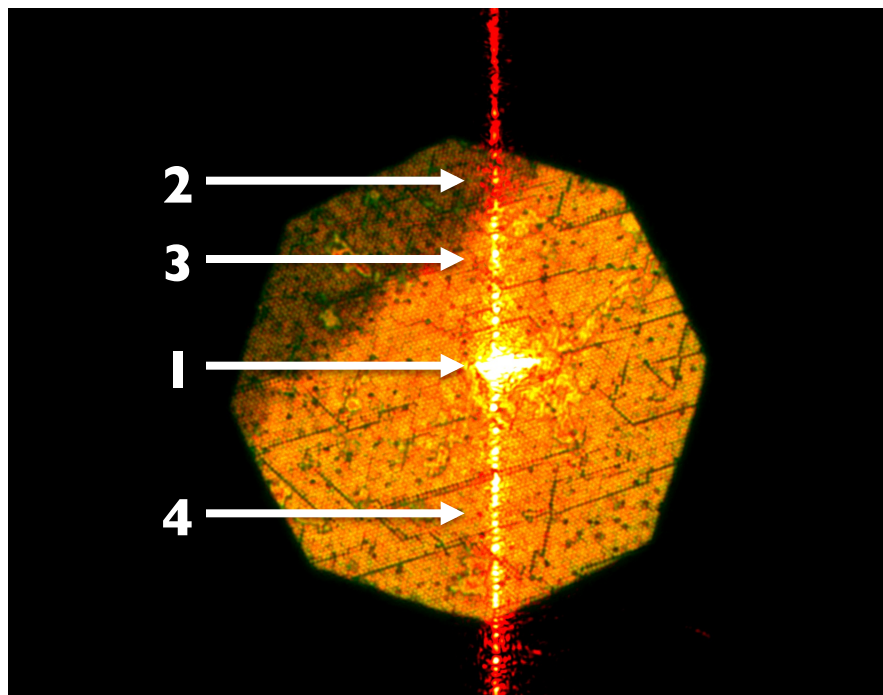


Raman of Gold vs Silicon



Raman Imaging

- Benzenethiol molecules on textured silver surface
- Illuminate to do one-dimensional chemical imaging along a line. Could also *scan* over the surface.



Chapter 2

Theoretical Considerations

2.1 The optical properties of materials

2.1.1 Maxwell's equations

All electromagnetic phenomena can be described, classically, by using Maxwell's equations. These foundational equations describe electromagnetic fields and how they evolve over time. In a region of space with no free charges or currents, these equations take the following form:

$$\nabla \cdot \mathbf{D} = 0 \quad (2.1)$$

$$\nabla \cdot \mathbf{B} = 0 \quad (2.2)$$

$$\nabla \times \mathbf{E} = -\frac{\partial}{\partial t} \mathbf{B} \quad (2.3)$$

$$\nabla \times \mathbf{H} = \frac{\partial}{\partial t} \mathbf{D} \quad (2.4)$$

where **E** (Volts per Meter) and **H** (Amperes per Meter) are the electric and the magnetic field intensities, respectively. In materials, the two other related parameters, **D** (Coulombs per square Meter) and **B** (Teslas), are the electric flux density and the magnetic flux density, respectively, where

$$\mathbf{D} = \epsilon \mathbf{E} \quad (2.5)$$

$$\mathbf{B} = \mu \mathbf{H} \quad (2.6)$$

and

$$\begin{aligned}\epsilon &= \epsilon_r \epsilon_0 \\ \mu &= \mu_r \mu_0.\end{aligned}$$

The fundamental constants $\epsilon_0 \approx 8.854 \times 10^{-12}$ (Farads per Meter) and $\mu_0 = 4\pi \times 10^{-7}$ (Henries per Meter) are the electric permittivity of free space and the magnetic permeability of free space, respectively. It is convenient to define ϵ_r , the relative electrical permittivity or dielectric constant, and the relative magnetic permeability μ_r , of the material. Since the research presented within this dissertation concerns non-magnetic materials operating at optical frequencies, we will only consider cases where $\mu_r = 1$ and $\mathbf{B} = \mu_0 \mathbf{H}$.

Under an applied electric field \mathbf{E} , the electrons within a material will respond according to equation (2.5), inducing an electric polarization density \mathbf{P} . For a linear material:

$$\mathbf{D} = \epsilon_r \epsilon_0 \mathbf{E} = \epsilon_0 (1 + \chi_e) \mathbf{E} = \epsilon_0 \mathbf{E} + \mathbf{P} \quad (2.7)$$

where χ_e is the electric susceptibility of the material, giving $\mathbf{P} = \epsilon_0 \chi_e \mathbf{E}$. These quantities describe the classical electromagnetic behavior of any given linear material.

2.1.2 Light: an electromagnetic wave

Famously, by combining equations (2.1) – (2.4), and assuming $\exp(-i\omega t)$ time-harmonic behavior, the resultant solution:

$$\mathbf{E}(\mathbf{x}, t) = \mathbf{E}_0 e^{i\mathbf{k} \cdot \mathbf{x} - i\omega t} \quad (2.8)$$

describes a wave with an angular frequency ω and a wavevector $\mathbf{k} = \omega/c \hat{\mathbf{k}} = k \hat{\mathbf{k}}$ propagating at a speed $c = 1/\sqrt{\mu_0 \epsilon_0}$, the speed of light in vacuum. The wavelength λ is related to the wavevector k via $k = 2\pi/\lambda$. The formula for $\mathbf{H}(\mathbf{x}, t)$ has a similar form. This establishes the fundamental identity of light as an electromagnetic wave. Furthermore, if the wave is propagating in a given material, then $\mathbf{k} = n\omega/c \hat{\mathbf{k}}$, where we have now defined a new quantity:

$$n \equiv \sqrt{\epsilon_r \mu_r} \quad (2.9)$$

which is the index of refraction of the material. In general, the optical properties of a given material are described by its index of refraction n and, since $\mu_r = 1$, by its dielectric function ϵ_r . These material properties may also vary with the frequency ω of the electromagnetic field, in which case the material would be described as being dispersive. Dispersion plays a significant role when describing the optical properties of metals, as discussed below.

Using the relationship $k^2 = k_x^2 + k_y^2 + k_z^2 = n^2(\omega/c)^2 = 4\pi^2n^2/\lambda^2$, it is possible to understand why dielectric structures cannot achieve subwavelength confinement: the x , y , and z components of the wavevector k cannot be increased arbitrarily. In fact, the electromagnetic wave cannot be confined to a region of space with a width smaller than $\approx \lambda/(2n)$, which is Rayleigh's resolution limit. Conversely, if this wave is propagating away from a sample through space in the “far-field”, i.e. as in a microscope, it cannot carry with it information about spatial scales less than $\approx \lambda/(2n)$, limiting the microscope's imaging resolution.

Mathematically, to beat these resolution limits, some components of \mathbf{k} must be imaginary, allowing the other components to increase arbitrarily and providing subwavelength confinement and information. With this situation, the wave no longer propagates in the direction of imaginary k and is called an “evanescent” wave. For instance, in a one dimensional example, if $k^2 = k_z^2 < 0$, then $E(z, t)$ from equation (2.8) becomes:

$$E(z, t) = E_0 e^{-|k|z} e^{-i\omega t}$$

which describes an exponentially decaying field with a penetration depth of $1/|k|$. Typically, the field penetration depths can be much less than the free-space wavelength λ . These high-resolution evanescent wave components also provide the “near-field” optical information about a sample. Gathering this information then requires probing the near-field, since wave propagation in free space into the far-field will filter this information.

As shown in the next section, a metallic material has $\Re[\epsilon_r] < 0$, providing one possible solution for the generation of such evanescent waves.

2.1.3 Dielectric function of a metal

Of course, equations (2.1) – (2.4) are also valid in regions where there are metallic interfaces. Understanding the optical properties of metals, therefore, requires modeling

its dielectric function ϵ_r . A simple oscillator model assumes that the metal consists of a gas of free electrons.^{34,35} Under the influence of an external time-varying electric field $\mathbf{E}(t)$, the position $\mathbf{x}(t)$ of an unbound electron with a mass m and charge e can be described as:

$$m\ddot{\mathbf{x}}(t) + m\gamma\dot{\mathbf{x}}(t) = -e\mathbf{E}(t) \quad (2.10)$$

where γ describes a viscous damping parameter related to the average time $\tau \equiv 1/\gamma$ between electron collisions. For an incident light wave, the driving field $\mathbf{E}(t)$ and the electron's response $\mathbf{x}(t)$ all vary sinusoidally as $\exp(-i\omega t)$. In this case, the time derivatives $\ddot{\mathbf{x}}(t)$ and $\dot{\mathbf{x}}(t)$ are simply replaced with $-\omega^2\mathbf{x}(t)$ and $-i\omega\mathbf{x}(t)$, respectively. The solution then becomes:

$$\mathbf{x}(t) = \frac{e\mathbf{E}(t)}{m(\omega^2 + i\gamma\omega)}.$$

The macroscopic electric polarization density $\mathbf{P}(t)$ then becomes:

$$\mathbf{P}(t) = -\frac{n_e e^2 \mathbf{E}(t)}{m(\omega^2 + i\gamma\omega)}$$

since $\mathbf{P}(t) = -n_e e \mathbf{x}(t)$ where n_e is the electron density. Using equation (2.7), we can now solve for $\mathbf{D}(t)$ and the dielectric constant $\epsilon(\omega)$:

$$\mathbf{D}(t) = \epsilon_0 \mathbf{E}(t) + \mathbf{P}(t) = \epsilon_0 \left(1 - \frac{\omega_p^2}{\omega^2 + i\gamma\omega}\right) \mathbf{E}$$

where we have defined a new quantity:

$$\omega_p \equiv \sqrt{\frac{n_e e^2}{\epsilon_0 m}} \quad (2.11)$$

which is called the “plasma frequency” of the metal, which describes the transition frequency from dielectric behavior to metallic behavior of the material. Finally, the dielectric function $\epsilon_r(\omega)$ of the metal is derived as:

$$\epsilon_r(\omega) = 1 - \frac{\omega_p^2}{\omega^2 + i\gamma\omega} \quad (2.12)$$

and depends only on the frequency of excitation ω and the two material-dependent parameters γ and ω_p . Equation (2.12) is the so-called “Drude” model.^{34,35} Using this with equation (2.9), it is possible to calculate the dispersive index of refraction $n(\omega)$ of

the metal. It should be noted that if equation (2.10), the original oscillator model, had instead assumed bound electrons that exhibit a characteristic resonant frequency ω_0 , we would have derived:

$$\epsilon_r(\omega) = 1 - \frac{\omega_p^2}{\omega^2 - \omega_0^2 + i\gamma\omega} \quad (2.13)$$

which is the so-called “Lorentz” model, describing materials that have specific absorption resonances. Both models are useful and accurately describe the optical properties of many materials. The imaginary part of $\epsilon_r(\omega)$ is related to the losses present in the material. These models are also directly incorporated into the numerical computer simulation algorithms described at the end of this chapter.

2.2 Plasmons

A plasmon is a collective oscillation of the free electrons.⁵ To derive $\epsilon_r(\omega)$, this oscillation was approximated with the equation of motion given in equation (2.10). At optical frequencies, $\omega \gg \gamma$ and equation (2.12) for $\epsilon_r(\omega)$ takes the approximate (lossless) form:

$$\epsilon_r(\omega) \approx 1 - \frac{\omega_p^2}{\omega^2} \quad (2.14)$$

which has three regions of interest: $\omega > \omega_p$, $\omega = \omega_p$, and $\omega < \omega_p$.

For $\omega > \omega_p$, then $\epsilon_r(\omega) > 0$ and the wavenumber k takes on a real value, allowing propagating electromagnetic waves according to equation (2.8). The metal behaves as a dielectric material.

For $\omega = \omega_p$, then $\epsilon_r = 0$ and $k = 0$, which means the oscillation has a constant phase across the metal. This describes the *volume plasmon* of the system, where all the free electrons are oscillating in phase at the plasma frequency. For a slab of metal, the opposing surface charges produce the restoring force for the harmonic oscillations. If the metal is semi-infinite, with only one surface exposed to air, the resonant frequency of the *surface plasmon* (SP) becomes $\omega_{sp} = \omega_p/\sqrt{2}$.³⁶ Furthermore, if the metal is in the shape of a small sphere surrounded by air, it can be shown that the resonant frequency of the *localized surface plasmon* (LSP) becomes $\omega_{lsp} = \omega_p/\sqrt{3}$. In these cases, the surface wave is not really propagating, and the electrons of the slab, surface, or small sphere are simply oscillating with the external electric field. The LSP resonances

are important when considering metallic nanoparticles, or when the metallic surface is highly curved or sufficiently rough.

For $\omega < \omega_p$, then k becomes complex, and equation (2.8) now describes a non-propagative evanescent field, i.e. one that decays exponentially into the metal. Incident light is reflected. It is within this regime, however, that a solution exists for *surface plasmon polaritons* (SPP) that propagate *along* the surface of the metal, with evanescent tails sticking into and out of the metal–dielectric interface.

2.2.1 Surface plasmon polaritons

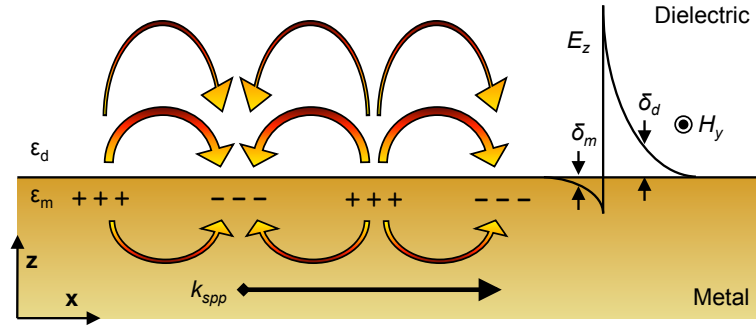


Figure 2.1: **Surface plasmon polaritons.** A surface plasmon polariton is a collective oscillation ($\omega \leq \omega_{sp}$) of the free electrons right at the surface of a metal–dielectric interface.³⁷ This oscillation has a wavevector k_{spp} and the fields decay exponentially away from the interface. The field penetration depth δ_d into the dielectric is greater than the penetration depth δ_m into the metal. The (transverse) magnetic field is entirely along the y axis.

Figure (2.1) shows a schematic of a surface plasmon polariton (SPP). The term *polariton* refers to the fact that the surface plasmon (SP), a polarization wave, is coupled with a photon. This means that the dispersion of light, i.e. the “light line,” crosses the surface plasmon resonance. To derive the SPP behavior, we first set the metal surface as the xy plane, with $z > 0$ being the surrounding dielectric. Starting with equation (2.8), it is assumed that the wave propagates in the x direction only. The magnetic field \mathbf{H} has only a y component, describing a *transverse-magnetic* wave. The wavevector is thus $\mathbf{k} = (k_x, 0, k_z)$, where k_z is imaginary. If ϵ_m is the dielectric constant of the metal

and ϵ_d that of the surrounding medium, appropriate boundary conditions specify that:

$$\frac{k_{z,m}}{\epsilon_m} = -\frac{k_{z,d}}{\epsilon_d}$$

and furthermore that:

$$k_{x,m} = k_{x,d} = k_x .$$

It is also known that

$$k_x^2 + k_{z,m}^2 = \epsilon_m \left(\frac{\omega}{c} \right)^2 \quad (2.15)$$

$$k_x^2 + k_{z,d}^2 = \epsilon_d \left(\frac{\omega}{c} \right)^2 \quad (2.16)$$

using the definition of the wavevector \mathbf{k} in each material. Solving these equations, the dispersion relation $k_x(\omega)$ is calculated as follows:

$$k_x(\omega) = k_{spp}(\omega) = \frac{\omega}{c} \left(\frac{\epsilon_d \epsilon_m}{\epsilon_d + \epsilon_m} \right)^{1/2} \quad (2.17)$$

giving the fundamental behavior of an SPP. The following assumptions about the two materials are made: $\epsilon_m = \epsilon'_m + i\epsilon''_m$, $|\epsilon'_m| > \epsilon''_m$, $\epsilon'_m < 0$, and $|\epsilon'_m| > \epsilon_d$. At optical frequencies, these conditions are easily achieved at a metal–dielectric interface. Three features of the surface wave now become apparent. First, the wavevector becomes complex, $k_{spp} = k'_{spp} + ik''_{spp}$, with real and imaginary components:

$$k'_{spp} = \frac{\omega}{c} \left(\frac{\epsilon_d \epsilon'_m}{\epsilon_d + \epsilon'_m} \right)^{1/2} \quad (2.18)$$

$$k''_{spp} = \frac{\omega}{c} \left(\frac{\epsilon_d \epsilon'_m}{\epsilon_d + \epsilon'_m} \right)^{3/2} \frac{\epsilon''_m}{2\epsilon'^2_m} . \quad (2.19)$$

The imaginary component of k_{spp} describes internal (ohmic) damping, giving the SPP a finite propagation length of $l_{ohm} = (2k''_{spp})^{-1}$, which is typically on the order of $\approx 10 \mu\text{m}$ for SPPs in the visible range on gold or silver.

Second, these conditions also imply that $k_{z,d}$ and $k_{z,m}$ are both imaginary, with $|k_{z,m}| > |k_{z,d}|$, and that the electromagnetic field decays exponentially from the metal–dielectric interface in the z direction, with characteristic decay lengths of $\delta_d = 1/|k_{z,d}|$ into the dielectric and $\delta_m = 1/|k_{z,m}|$ into the metal. The field is therefore maximum

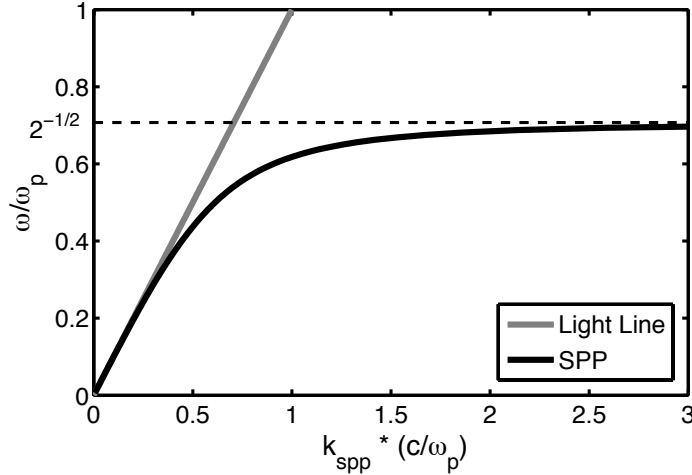


Figure 2.2: Dispersion relation of surface plasmon polaritons. Plotting equation (2.17) shows that the momentum (wavevector) of a surface plasmon polariton is always greater than free-space light. For small ω/ω_p , k_{spp} lies very close to the light line, and the polariton is “light-like.” For $\omega/\omega_p \rightarrow 1/\sqrt{2}$, the polariton approaches the surface plasmon resonance, and becomes more “plasmon-like” with a very large momentum. The dielectric function of the metal in this plot was set to be lossless as given in equation (2.14). If loss is considered, k_{spp} will not diverge but will approach a maximum value at the surface plasmon frequency.

at the surface, giving high sensitivity to surface properties. Given equations (2.15) and (2.17), the distance at which the field falls to $1/e$ becomes:

$$\delta_d = \frac{\omega}{c} \left(\frac{\epsilon'_m + \epsilon_d}{\epsilon_d^2} \right)^{1/2} \quad (2.20)$$

$$\delta_m = \frac{\omega}{c} \left(\frac{\epsilon'_m + \epsilon_d}{\epsilon'_m^2} \right)^{1/2} \quad (2.21)$$

For a free space wavelength of 600 nm, $\delta_d \approx 390$ nm and $\delta_m \approx 24$ nm for silver, whereas $\delta_d \approx 280$ nm and $\delta_m \approx 31$ nm for gold.³⁷ The spatial extent of the field directly influences the sensitivity to thin films adsorbed on the surface.

Third, an SPP always lies to the right of the “light-line,” illustrated in figure (2.2), since $k'_{spp} > (\omega/c)(\epsilon_d)^{1/2}$, giving SPPs a greater in-plane wavevector than free-space light. This has implications for the experimental generation of SPPs. Since momentum

must be conserved, the SPP will not radiate into free-space light. Conversely, it is not possible to excite the SPP wave on a flat metal surface with free-space light. At a given angular frequency ω , this momentum must be accounted for in order to generate the surface plasmon polaritons with incident light. This is typically achieved with a grating or prism coupler, illustrated and explained in figure (2.3). A single bump, groove or defect will also provide sufficient coupling.

It is this characteristic dispersion relationship that gives SPPs their utility in nanotechnology: it is possible to have an electromagnetic surface wave with very tightly confined energy ($\delta_d \approx 100$ nm) and large wavevectors all at optical frequencies. As described earlier, since k_z is imaginary and $k_z^2 < 0$, the relation $k_x^2 + k_y^2 - |k_z|^2 = n^2(\omega/c)^2$ implies that k_x and k_y can now be increased arbitrarily, leading to ever-greater confinement. Dielectric waveguides cannot achieve this subwavelength confinement of optical energy. Metallic nanostructures, such as nano-sharp tips, nano-scale holes, and subwavelength-scale patterning, can exert control over the flow of electromagnetic energy on unprecedented length scales. Due to such tight confinement of the optical energy, plasmonic structures are highly sensitive to surface properties. This is especially useful, in the context of the research presented here, for detecting the presence and signature of adsorbed molecules. In this dissertation, SPPs are explored for their utility in different sensing environments.

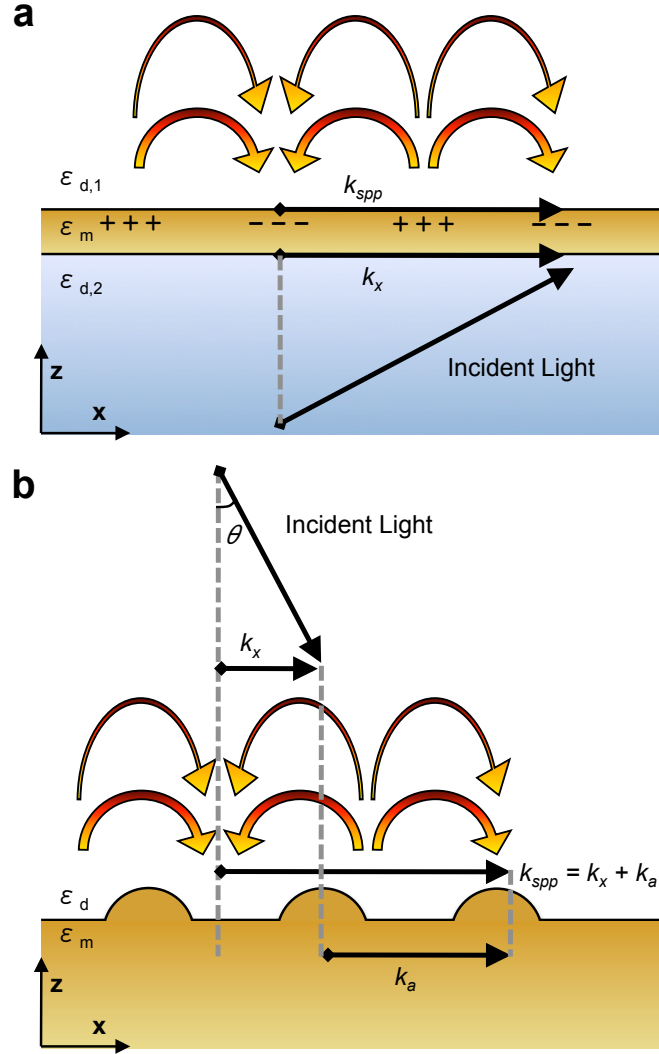


Figure 2.3: Surface plasmon polariton coupling geometry. (a) Using a thin metal film, and illuminating from below when $\epsilon_{d,1} < \epsilon_{d,2}$ in a total internal reflection mode to generate evanescent surface waves, the in-plane wavevector k_x of the incident light will match k_{spp} on the other side of the film at a given angle, exciting an SPP and resulting in a sharp dip in reflected intensity. This is the so-called “Kretschmann” configuration.³⁸ (b) The in-plane wavevector $k_x = (2\pi/\lambda) \sin \theta$ can also be augmented by the spatial frequency wavevector $k_a = 2\pi m/a$ of a surface grating with period a and grating order m , providing enough momentum to excite k_{spp} . A single bump, groove or defect will also provide sufficient momentum, due to its large distribution of spatial frequencies.

Chapter 6

Surface Enhanced Raman Spectroscopy and Plasmonics

Real-time, label free SPR biosensing is a very useful technique, but it does not give any *chemical* information. Only refractive index changes are recorded, meaning that non-specific binding events can be an issue. As discussed in Chapter 1, Surface Enhanced Raman Spectroscopy (SERS) also relies on the excitation of plasmon resonances, and is a powerful method for identifying proximate molecules.^{6,8–10,143} Indeed, single-molecule sensitivity has been reported,¹⁴⁴ promising to make SERS techniques as broadly applicable as fluorescence. Since the bound molecules are effectively “fingerprinted,” SERS detection naturally complements the label-free methods of SPR biosensing. For example, SERS has recently been used to detect trace amounts of antrax,¹⁴⁵ nuclear waste,¹⁴⁶ and pesticides.¹⁴⁷ Additionally, since a SERS signal is dependent on the efficient excitation of plasmon resonances, it can also be used as a tool for characterizing a plasmonic device, for example, by pinpointing the locations and the intensities of maximum field enhancement.

6.1 Theoretical Foundation

Raman scattering itself is a very “feeble”⁷ phenomenon, many orders of magnitude weaker than fluorescence.⁹ However, Raman spectroscopy has several important advantages, in that it is a vibrational spectroscopy technique, unlike fluorescence, providing

much more information about molecular structure and orientation. It is also a complementary technique to infrared absorption spectroscopy.⁹

6.1.1 Classical Raman Model

Raman spectroscopy can be understood classically or quantum mechanically. Classically, we will consider a single diatomic molecule oriented along the z axis. Following the derivation presented in Van Duyne et al.,⁶ in an external electric field $E(t) = E_z \cos(\omega_0 t)$ oscillating along the z axis with an angular frequency ω_0 , the z -component of the polarization of the molecule $\mu_z(t)$ will change with time according to:

$$\mu_z(t) = \alpha_z E_z \cos(\omega_0 t)$$

where α_z is electric polarizability of the molecule. In three dimensions, the polarizability is typically a second-rank tensor with nine components. If the molecule is in turn vibrating on its own with an angular frequency of ω_v , the polarizability will now depend (linearly) on the offset $\Delta r(t)$ from the equilibrium inter-nuclear distance, becoming:

$$\alpha_z = \alpha_z^0 + \frac{d\alpha_z}{dr} \Delta r(t)$$

where α_z^0 is the equilibrium polarizability, and $\Delta r(t) = \Delta r_{max} \cos \omega_v t$. Combining these two relations, and the time-dependence of both α_z and μ_z , the polarizability of the molecule fluctuates in time as:

$$\begin{aligned} \mu_z &= \alpha_z^0 E_z \cos \omega_0 t \\ &+ \frac{1}{2} \frac{d\alpha_z}{dr} \Delta r_{max} E_z \cos(\omega_0 + \omega_v) t \\ &+ \frac{1}{2} \frac{d\alpha_z}{dr} \Delta r_{max} E_z \cos(\omega_0 - \omega_v) t . \end{aligned}$$

Each of the three components of this equation is an oscillating dipole, which will re-radiate the incident light. The oscillation at ω_0 is the same frequency as the incident light, and is inelastic *Rayleigh* scattering. The oscillation at a higher frequency $\omega_0 + \omega_v$ is *anti-Stokes Raman* scattering, and the oscillation at a lower frequency $\omega_0 - \omega_v$ is *Stokes Raman* scattering. It is with this Raman scattered light that information about the vibrational modes ω_v of the molecule can be probed.⁶

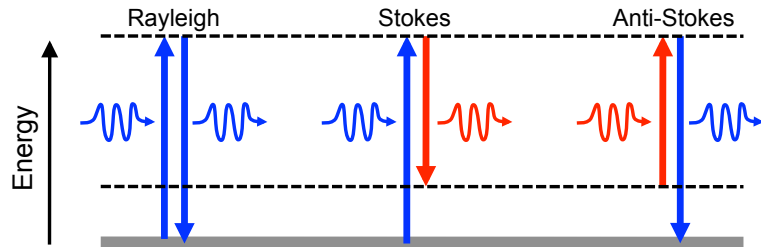


Figure 6.1: **Quantum mechanical picture of Raman scattering** An incoming photon (from the right) will scatter either elastically with the same energy (Rayleigh), or inelastically with either a lower energy (Stokes Raman) or with a higher energy (anti-Stokes Raman). The extra energy is either given by or absorbed by the excitation of a molecular vibrational mode.

6.1.2 Quantum Mechanical Raman Model

Quantum mechanically, an incoming photon with an energy $\hbar\omega_0$ will scatter either elastically (with the same energy) or inelastically (with an altered energy) from the molecule. This is viewed as a two-photon process. First, the photon excites the molecule to a short-lived, higher-energy state. After a very short time, the energy is released in the form of another scattered photon, and the molecule returns a state that conserves total energy. For instance, if the scattered photon has a lower energy than the incoming photon, the molecule will have absorbed an amount of energy $\hbar\omega_v$ related to one of its vibrational states. The scattered photon will then have an energy of $\hbar(\omega_0 - \omega_v)$, as with Stokes Raman scattering. The process for anti-Stokes Raman scattering involves the scattered photon having an energy of $\hbar(\omega_0 + \omega_v)$, with the molecule having lost a quantum of vibrational energy equal to $\hbar\omega_v$. This type of scattering is typically much weaker, since the molecule would have to be in a (more unlikely) higher energy state when hit by the photon. These processes are outlined in figure (6.1). In this way, both the classical and the quantum mechanical pictures allow a scattered beam of light or stream of photons to have altered frequencies in a way specific to the vibrational modes of the molecule. As an example, the Raman spectrum of benzenethiol (BZT) is presented in figure (6.2). The Raman spectrum, and typically only the stronger Stokes spectrum, is presented in units of cm^{-1} , and represents a *shift* from the incident light.

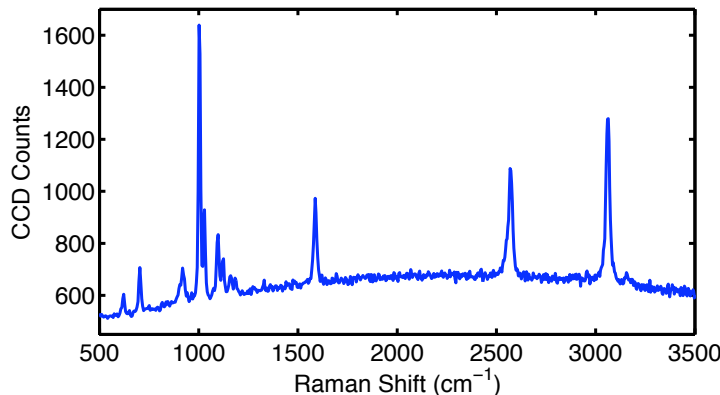


Figure 6.2: Raman spectrum of benzenethiol. A Raman spectrum presents a series of sharp peaks, each one corresponding to different vibrational modes, or “fingerprints” of the molecule. For example, the strong peak at 1002 cm^{-1} corresponds the in-plane C-C-C bending mode of the benzene ring. Data taken with neat 1mM benzenethiol and the confocal Raman setup described further below.

6.1.3 Surface Enhanced Raman Spectroscopy

Unfortunately, Raman scattering is typically very weak, with a cross section roughly 10^{14} times weaker than fluorescence. However, when a molecule is very near to a roughened or nanostructured noble metal substrate, the Raman signal can be greatly increased,⁸ usually around 10^4 to 10^8 times.⁹ This phenomenon is known as Surface Enhanced Raman Spectroscopy (SERS) and carries both a “chemical” enhancement¹⁴⁸ of roughly 10–100 times, and an “electromagnetic” enhancement due to the excitation of plasmon resonances and large field intensities in and around the nanostructured noble metal substrate.⁶

Chapter 2 introduced *localized surface plasmon resonances*, or LSPR. Since SERS occurs on roughened metallic substrates, we can understand the enhancement by modeling the roughness as small metallic *nanoparticles*, whose diameters are much smaller than the wavelength of the incident light. Under the influence of an external electromagnetic field, the electron plasma of a metallic nanoparticle will oscillate, enhancing the local field. The field amplitude enhancement of a spherical metal nanoparticle can

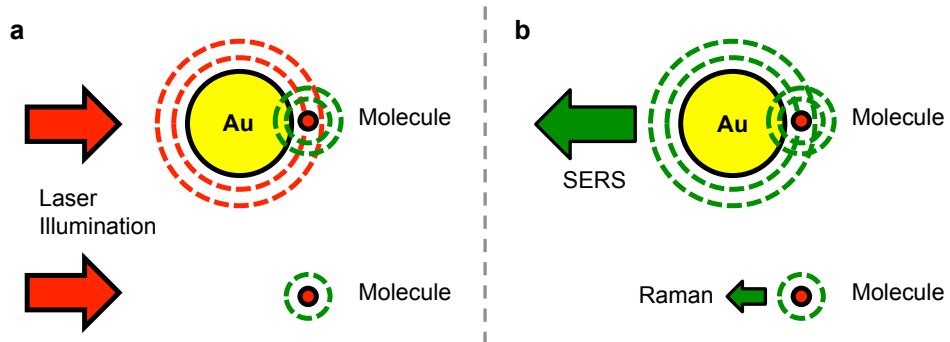


Figure 6.3: Surface enhanced Raman spectroscopy mechanism. A gold nanoparticle will enhance both (a) the incident field, as well as (b) the scattered field, greatly boosting the Raman signal from a proximate molecule. Since the intensity is enhanced twice, the SERS signal is proportional to intensity squared.

be expressed as:

$$\text{Enhancement} = \frac{\epsilon_m - \epsilon_d}{\epsilon_m + 2\epsilon_d} \left(\frac{R_{np}}{R_{np} + D} \right)^3 \quad (6.1)$$

where ϵ_m and ϵ_d are the permittivities of the metal nanoparticle and the surrounding dielectric medium, respectively, R_{np} is the radius of the nanoparticle, and D is the distance from the surface of the nanoparticle. This enhancement is especially strong on resonance, when $\Re(\epsilon_m) = -2\epsilon_d$.

Due to such a strong field, the Raman signals are enhanced by many orders of magnitude. In fact, the nanoparticle boosts the signal in two ways. First, the incident field is localized and intensified by the nanoparticle, increasing the field seen by the Raman-active molecule. Second, the scattered light, i.e. the Raman spectrum, is localized and intensified in turn by the nanoparticle. Even though the Raman light is frequency-shifted from the incident light, the resonance of the nanoparticle is sufficiently wide to enhance both the incoming and scattered fields. Thus the SERS signal is proportional to the incident field intensity *squared*, i.e. the SERS Enhancement Factor (EF) is proportional to the electric field to the fourth power. This process is outlined in figure (6.3). Additionally, the SERS enhancement drops off very quickly with the distance, D .

By raising equation (6.1) to the fourth power, we see that

$$EF \propto \left(\frac{R_{np}}{R_{np} + D} \right)^{12}$$

meaning that molecules only within a few nanometers from the surface contribute a strong SERS signal.

To quantify the enhancement, the SERS signal must be compared to a normal, bulk Raman signal. Typically, the intensity of a single Raman peak I_{bulk} is compared to the intensity I_{sers} of the identical SERS peak. Additionally, the number of molecules, or scatterers, must be accounted for. Therefore, the enhancement factor is calculated as follows:

$$EF = \frac{I_{sers} N_{bulk}}{I_{bulk} N_{sers}} \quad (6.2)$$

where N_{bulk} are the number of molecules illuminated in the bulk, giving a normal Raman signal, and N_{sers} are the number of molecules illuminated on the roughened metallic substrate, giving the SERS signal. For accurate calculations of EF , N_{sers} must be estimated knowing the packing density of the molecules, and the surface area of the metal.

6.2 Engineering plasmonic SERS substrates

As we have seen, the local enhancement of the optical field is a primary factor for a strong SERS signal.¹⁰ However, the measurements are typically performed on roughened or randomly structured metallic substrates with poor control over the location and intensity of the enhanced fields, or “hot spots.”¹⁴⁹ A SERS substrate that is both highly reproducible and that can offer high signal enhancement due to controlled field localization can offer immediate benefits to a broad range of disciplines where efficient and accurate chemical detection is necessary.

Since the EOT effect through a nanohole array in a thin gold or silver film will excite plasmon resonances, it is expected that the SERS signal may also be quite high.¹⁵⁰ Using the Raman microscope system described by Bantz and Haynes,¹⁵¹ figure (6.4) shows a sample SERS spectrum of benzenethiol (BZT) molecules extracted from a silver film with and without nanohole array patterning. The silver films was first incubated in a 1 mM solution of BZT in ethanol for 24 hours, forming a well-defined self-assembled

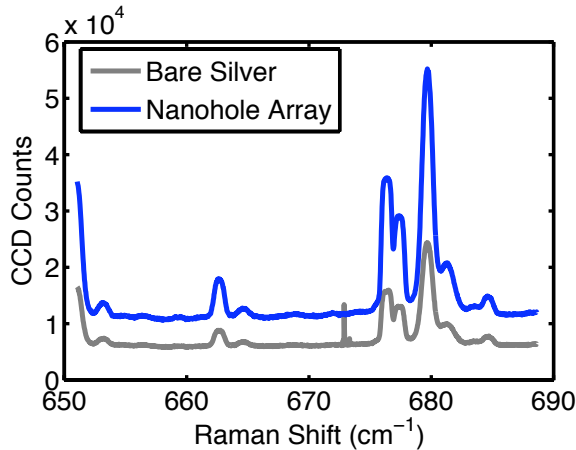


Figure 6.4: **Nanohole arrays and SERS.** A silver film with adsorbed benzenethiol molecules will have some SERS activity, but the signal will increase with nanohole array patterning. Nanohole arrays and the EOT mechanism provide many design freedoms, allowing the SERS substrate to be tuned for maximum enhancement.

monolayer of molecules. Given a packing density¹⁵² of 6.8×10^{14} molecules/cm² and an estimate of the surface area, EFs can be calculated via equation (6.2). The rough silver film exhibits some SERS activity, which can be enhanced with patterning. In fact, nanohole arrays are also *tunable*, with their periodicity, providing a degree of freedom for maximizing the EF. Using double-hole arrays, LSPR may be excited as shown in figure (4.7) on page 40, also making them good candidate SERS substrates.¹²¹ The possibility of using simple nanohole arrays as a well-defined and efficient SERS substrate indeed shows promise. Beyond this, other SPP optical elements may also provide free design parameters, such as the incorporation of the surrounding Bragg mirrors demonstrated in Chapter 5.

To further characterize these types of samples, a scanning confocal Raman microscope system (WITec Alpha300R™) is used, capable of providing high-resolution chemical mapping and SERS imaging of nanohole arrays, matrices of sensor spots, or other plasmonic devices. The confocal system can be used to directly measure EFs, or simply to map the locations and relative intensities of the SERS hot spots, giving information about the distributions of the intense SPP fields. Figure (6.5) shows a schematic of the

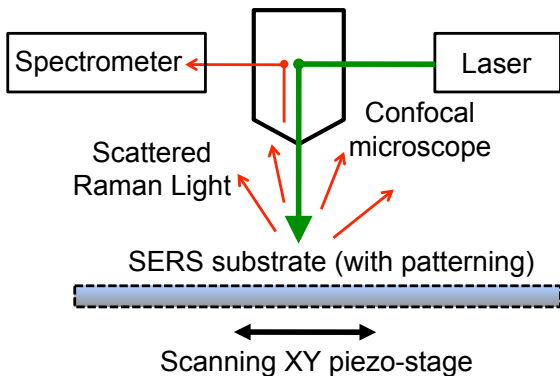


Figure 6.5: Scanning confocal Raman microscope. A confocal microscope illuminates a substrate with a diffraction-limited laser spot. By scanning the focus over the sample in x and y , a high-resolution chemical map of the surface can be obtained. At each spatial coordinate, a complete Raman spectrum is collected. Intensity images may then be generated by plotting the height of a specific Raman peak as a function of x and y . The system may also be used for plasmonic device characterization, as SERS hot spots will show the locations of high electric fields. By changing the focal distance in z , three-dimensional information can also be obtained. The spatial resolution is approximately $\lambda/2$ in x and y , and λ in z , where λ is the wavelength of the laser.

system. As the laser beam is scanned over the SERS substrate, a Raman spectrum is stored for each location. Intensity maps can then be generated by extracting the height of a specific Raman peak as a function of position. Figure (6.6) show an intensity image of a 3-by-3 matrix of nanohole arrays, each with a different periodicity. In this case, the sample was incubated in standard rhodamine 6G (R6G) dye molecules, typically for 24 hours to form a well-defined molecular monolayer. The excitation wavelength was 514 nm. Figure (6.7) shows a SERS intensity map of an array of double holes.¹²¹ Figure (6.8) shows SERS data from a 2-by-2 matrix of nanohole arrays with Bragg mirrors.

To further develop practical plasmonic SERS substrates, novel large-area fabrication methods such as colloidal self-assembly can be used.¹⁵³ Also, controlling the orientation and critical dimensions of metallic nanogap structures shows promise for high-efficiency SERS substrates.¹⁵⁴ However, as shown, roughness can have a profound effect on the quality of the SERS substrate. The next chapter presents a novel fabrication scheme that is capable of producing high-quality, ultrasmooth, patterned metallic substrates.

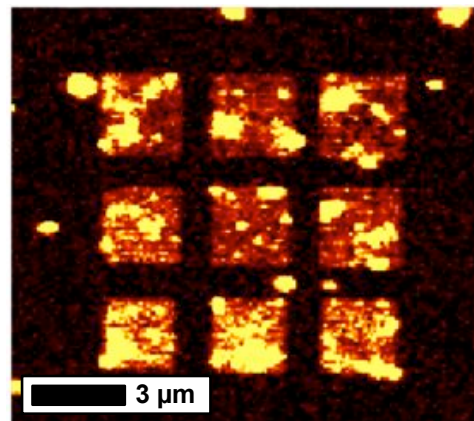


Figure 6.6: **Confocal Raman scans of nanohole arrays.** A 3-by-3 matrix of nanohole arrays with different periods allows imaging of the plasmonic resonances. The bottom row of nanohole arrays gives the highest and most homogeneous SERS signal. Due to the roughness of the silver film, randomly located hot spots are also generated.

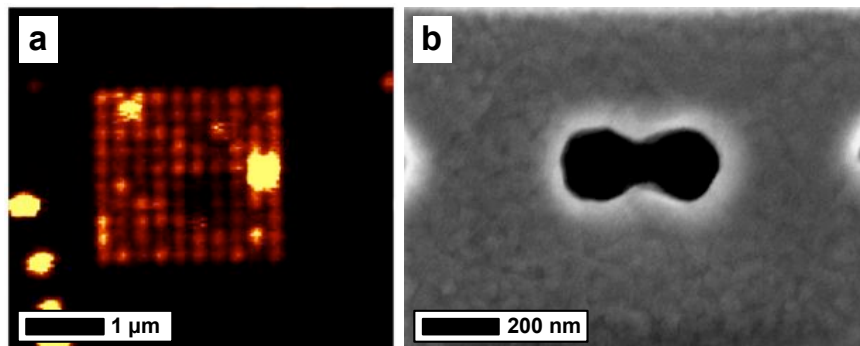


Figure 6.7: **Confocal Raman scans of double-hole arrays.** (a) SERS intensity map of a (b) double-hole array. Double-hole arrays generate LSPR, also making them good candidates for SERS substrates.

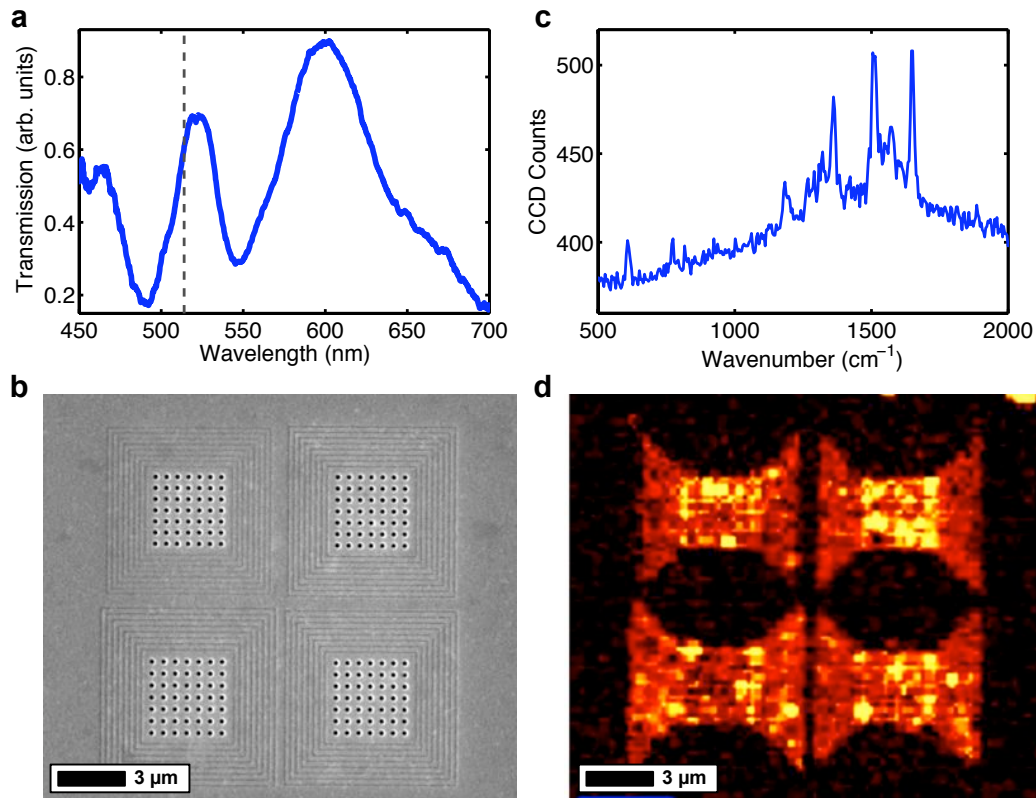


Figure 6.8: Confocal Raman scans of nanoholes with Bragg mirrors. (a) Tuning the periodicity of a nanohole array with surrounding Bragg mirrors to give maximum transmission and maximum SPP fields near the 514 nm laser excitation, marked by the vertical dash. (b) A 2-by-2 matrix of arrays. The nanoholes each have a diameter of 180 nm, and the multiple arrays have periodicities that range from 400 nm to 480 nm to find the best tuning conditions using a fixed excitation wavelength of 514 nm. The wavelength of maximum SPP field and enhanced Raman is, to first order, a function of the periodicity of a nanohole array, given in equation (3.1). (c) A Raman spectrum of R6G dye molecules taken from a single spot within the nanoholes. (d) An intensity image is made by mapping the height of a specific peak. The surrounding Bragg grooves are also seen, with a horizontal excitation polarization, since they also introduce a SERS-active “roughness.” The top right array shows the most enhanced and homogeneous SERS signal. However, due to fabrication roughness, the SERS intensity varies both inside the nanohole array regions and outside.